Plastic Deformation, Failure and Energy Absorption of Sandwich Structures with Metallic Cellular Cores

Feng Zhu[1], Guoxing Lu[2,*], Dong Ruan[3], Zhihua Wang[4]
[1]Bioengineering Center, Wayne State University, Detroit, MI 48201, USA
[2]Corresponding author, School of Mechanical and Aerospace Engineering, Nanyang Technological University, Singapore 639798, Singapore
[3]Faculty of Engineering and Industrial Sciences, Swinburne University of Technology, Hawthorn, VIC 3122, Australia
[4]Institute of Applied Mechanics and Biomedical Engineering, Taiyuan University of Technology, Taiyuan 030024, China

Received on 13 Sept 2010, Accepted on 2 Oct 2010

ABSTRACT
Cellular metals with stochastic, 2D or 3D periodic microstructures can sustain large plastic deformation at almost constant stress. Due to such excellent energy absorption capability, cellular metals are very suited to be used as the core of sandwich structures, which have been applied widely to the areas of aerospace and aeronautical design, the automotive manufacturing, and shipbuilding, as well as the defense and nuclear industries. Although there is a great deal of research currently available related to the behaviour of sandwich structures with metallic cellular core under various loading conditions, they are widely scattered in the literature. This review paper brings together the latest developments in this important research area. Three types of cellular metals, namely metal foams, honeycombs and prismatic materials and truss and textile based lattice materials are considered. The responses of sandwich structure with such cores subjected to different loads, i.e. quasi-static/low velocity compression and indentation, ballistic impact, high speed compression and blast loading, are reviewed. The emphasis has been placed on their plastic deformation, failure and energy absorption behaviours.

Key words: Sandwich Structures, Cellular Materials, Plastic Deformation, Failure, Energy Absorption

1. INTRODUCTION

Over the past decade, a variety of metallic and polymeric cellular materials have been produced with the aim of developing lightweight structures (mainly sandwich structures) which are adequately stiff and strong. These cellular materials can be thought of porous composites made up of solid and space connected with plates, shells or struts. Due to their light weight, high specific strength, high specific toughness and good energy dissipating

*Corresponding author. E-mail addres: GXLu@ntu.edu.sg

properties, cellular materials are frequently used as the core of sandwich structures, where the face-sheets provide the structure with higher bending and stretching strength, and the core sustains indentation or crushing mainly. Now sandwich structures have been increasingly used in a wide range of applications, such as vehicle, aircraft, ship manufacturing, packaging and defense industries [1].

Based on the geometries and topologies of the microstructures, cellular materials can be classified as those with stochastic cells and periodic cells. The first type of materials, including open and closed cell metallic foams, have random microstructures; while in the second type of materials, the microstructures are periodic: either two-dimensional channels (honeycombs and prismatic materials) or three-dimensional truss or textile based assemblies. A hierarchical description of cellular materials classification is shown in Figure 1. As synthetic polymer foams are now a mature industry and well documented in many technical publications, in this paper, the review is mainly concentrated on the metallic cellular materials.

- Metal foams
  A metal foam is a cellular structure consisting of a solid metal - frequently aluminum - containing a large volume fraction of gas-filled pores. The pores can be sealed (closed-cell foam), or they can form an interconnected network (open-cell foam). The defining characteristic of metal foams is a very high porosity: typically 75–95% of the volume consists of void spaces. The strength of foamed metal possesses a power law relationship to its density; i.e. 20% dense material is more than twice as strong as 10% dense material. The mechanical properties and fabrication state-of-arts of the metal foams have been extensively studied and documented in [2–4].
- Honeycombs and prismatic materials
  Honeycombs are composed of plates or sheets that form the edges of unit cells. These can be arranged to create triangular, square, hexagonal or circular shapes. Their unit cells are repeated in two dimensions to create a cellular solid. The mechanics and manufacturing methods were introduced in [2, 5]. If the cores of honeycombs are

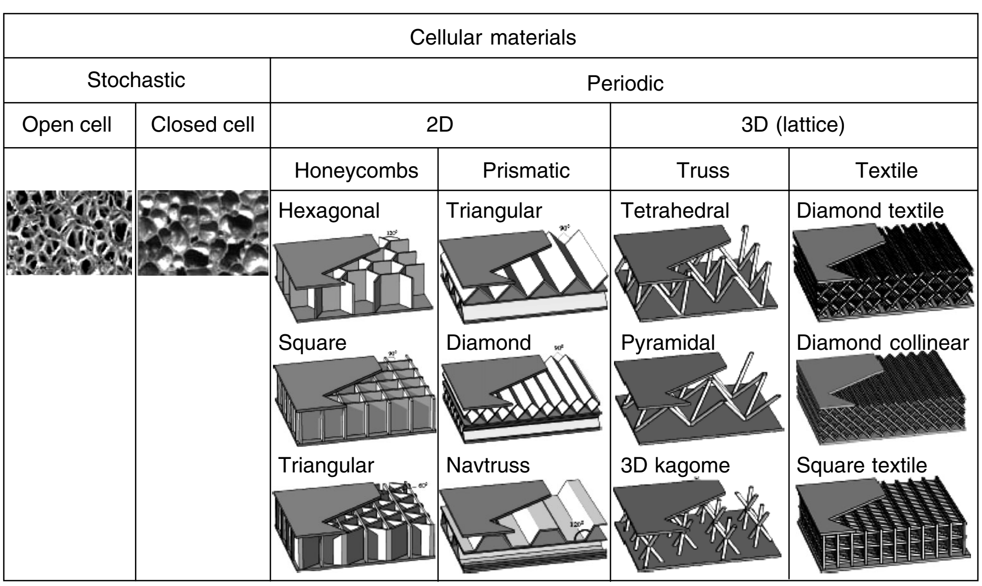

Figure 1. Hierarchical description of cellular materials classification, where the cellular material with stochastic or periodic microstructures is configured as the cores of sandwich panel structures (2, 6)

rotated 90° about their horizontal axis, they become prismatic structures with open (easy flow) cells in one direction and a closed cell structure in the two orthogonal directions. The 2D periodic channels can be used as cross flow heat exchangers.

- Truss and textile based lattice materials
  These two types of materials are 3D open cell structures. The truss based lattices have several struts each meeting at a node, while the textile based structures are composed of layers of a plain weave metal wires that have been bonded to each other.

Overviews of the recent developments in topology design and the fabrication of novel periodic cellular metals can be seen in [6–9]. Cellular materials are characterised by the solid of which they are made, by their relative density $\bar{\rho}$, and by the cell topology, i.e. the connectivity and regularity of the cell walls and edges. Microstructural models [2, 10, 11] were proposed and micro-scale modelling [12] were carried out to quantitatively describe the relationship between stress and strain for cellular materials. Deshpande et al. [10] distinguished the characteristics of cellular materials as bending-dominated where a few struts undergo significant bending or torsion, and stretching-dominated with their struts mainly enduring compression or tension. Gibson and Ashby [2] demonstrated that the strength of closed cell foams scales as $\bar{\rho}^{1.5}$ when their cell walls are governed by bending. Deshpande et al. [10] found that the strength of cellular solids scales as $\bar{\rho}$ when their cell walls are governed by stretching. Stretching-dominated structures can be stronger than traditional foam materials, which are most bending-dominated. However, unlike the bending-dominated foams, in compression the stretching- dominated material have a softening post-yield response due to the buckling of the struts. Thus, these materials may be less attractive as energy absorbers since this application requires a stress-strain response with a long, flat plateau [10].

More recently, the attention of academia and industry has turned to the multifunctional performance of cellular materials and structures. For example, Figure 2 shows a typical application of cellular-core sandwich structures in automobile industry, with each circle representing an individual area, i.e. ultra-light structures, energy absorbers and heat and sound dissipation media.

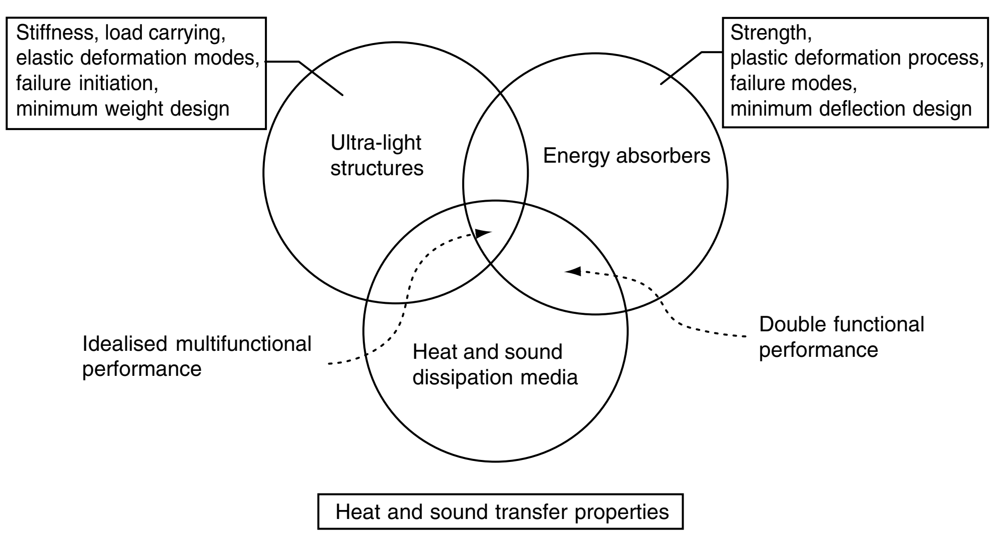

Figure 2. A typical application of cellular-core sandwich structures in automobile industry

In this paper, our focus will be placed on the performance of cellular-core sandwich structures used as energy absorbers, mainly including the post-yielding behaviour of the materials, their plastic deformation process, failure modes and the associated energy dissipating behaviours. The mechanical properties within the elastic limit, such as stiffness, elastic deformation modes and vibration are beyond the scope of this paper. The performances of cellular-core sandwich structures are discussed in terms of quasi-static/low velocity impact, high speed ballistic and blast loading conditions. Unlike conventional structures which undergo only small elastic deformation, the protective structures used as energy absorbers have to sustain extreme loads, so that their deformation and failure may involve large geometry changes, strain-hardening effects, strain-rate effects and various interactions between different deformation modes such as bending and stretching. The elastic behaviour of sandwich panels at small deflections has been extensively studied and well documented in several technical books [13–16]. But their plastic deformation and its associated energy-absorbing behaviour, especially when deflections are large, are relatively less investigated. The related work in this area is summarised in this review paper.

2. QUASI-STATIC AND LOW VELOCITY IMPACT PERFORMANCE

2.1. SANDWICH BEAMS

The quasi-static deformation mechanism of sandwich beams is usually tested by 3-point or 4-point bending, and investigations generally concentrate on (1) structural failure modes and (2) initial load for initial plastic collapse. The sandwich beams may have composite (e.g. E-glass/Epoxy or Carbon/Epoxy) [17–26] or metallic skins [27–33] and a polymeric/metallic foam core. Their typical failure modes under 3-point bending are shown in Figures 3(a) and (b), respectively. It has been found that the competing collapse modes of sandwich beams are correlated to their physical and geometric properties (core relative density, core thickness, face thickness and strength, cellular morphologies, etc.) and boundary conditions.

Compared with the face sheets made from elastic-brittle solids such as composite laminates, the ductile metallic faces allow large plastic deformation. i.e. global bending and stretching and thus they can produce much higher load and dissipate energy. Tagarielli and Fleck [32] experimentally and theoretically studied the effect of simply supported and fully clamped boundary conditions of sandwich beams on their behaviours at finite deflections. The specimens have annealed aluminium skins and an aluminium foam core bonded together

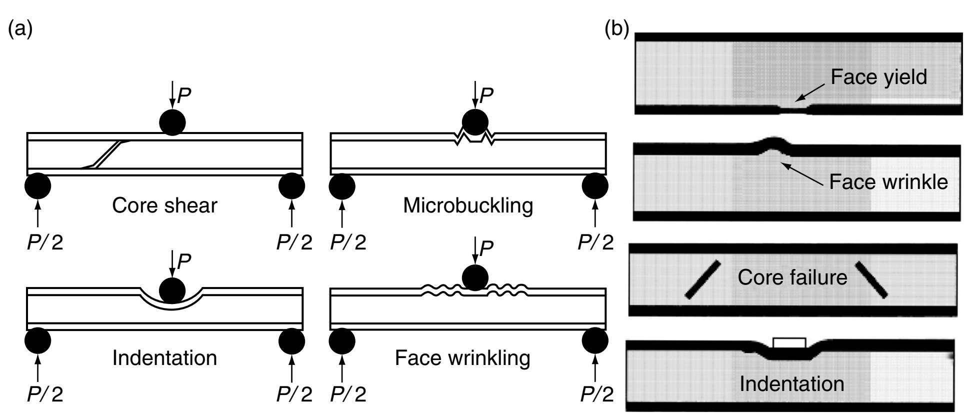

Figure 3. Failure modes of sandwich beams: (a) composite skins (24); (b) metallic skins (27)

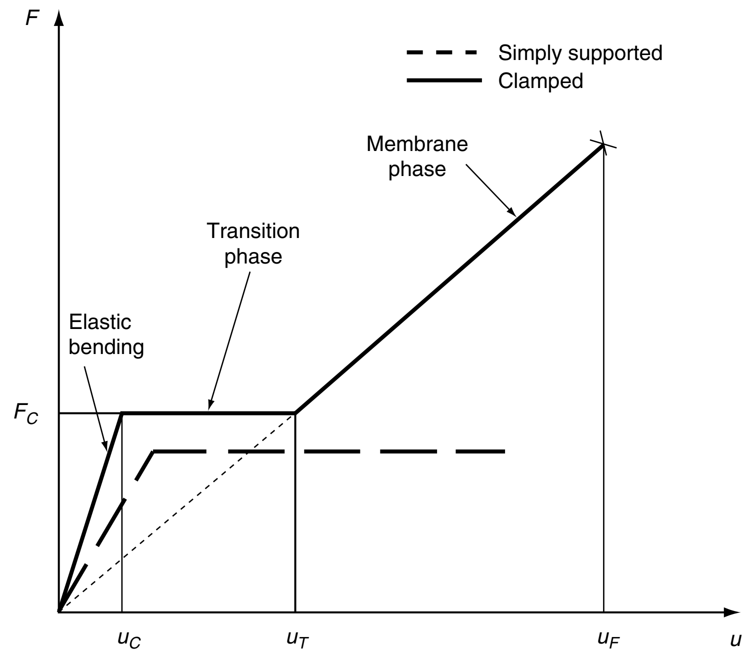

Figure 4. Stages of collapse of simply supported and clamped sandwich beams (32)

by Redux 322 epoxy adhesive. The load versus deflection response of the beams may be subdivided into three phases, as sketched in Figure 4.

Simply supported beams undergo continued plastic collapse at nearly constant load; eventually, the transverse deflection becomes sufficiently large that the structure fails by fracture of the face sheets or core. In contrast, clamped beams undergo membrane stretching of the face sheets beyond initial yield, and this gives rise to a hardening macroscopic response. Initial plastic collapse of clamped sandwich beams occurs by face yield, core shear, or indentation at small transverse deflections. Subsequent transverse deflection, however, involves tensile stretching of the faces and core. The stress distribution within the beam evolves from that associated with the initial collapse load to that of pure membrane action, with the membrane solution achieved when the deflection is about equal to the thickness of the beam. Thereafter, the beam deforms in a membrane mode, and yields axially until the face sheets tear when the axial plastic strain attains the material ductility. Equilibrium considerations give an expression for the load (F) versus deflection (u) in the membrane phase as

$$F(u) = \frac{8tb\sigma_f}{l-a}u \tag{1}$$

where b is width of the beam; t is face thickness; a is width of a flat-ended punch, σ_f is yield strength of the skin material. It is assumed that the deflection u is small compared with the span l, and that the net axial force in the faces is much greater than that in the core. Based on the similar procedure, Qin and Wang [34] proposed another analytical solution for large deflections of fully clamped and simply supported slender sandwich beams with a metal foam core loaded by a flat punch; a unified yield criterion was used for the metallic sandwich cross-sections with various core strengths and geometries. Moreover, the effects of punch size and the boundary conditions were discussed as well.

Yu et al. [35] studied the low-velocity impact behaviour and failure mechanism of aluminium face sheet/open cell aluminium foam core sandwich beams. It was found that the crush load under impact loading is larger than that under quasi-static loading but the energy absorption is reduced. Since the face sheet and core thickness investigated was in a narrow range, they found that the beams fail mainly by a face yield mode. No significant strain rate sensitivity at low impact speeds has been found in the tests, which is consistent with that obtained by Crupi and Montanini [30]. Cantwell and co-workers [36–40] carried out low velocity tests on the sandwich beams made of a wide range of materials, and a large number of different failure modes have been obtained. For instance, shear fracture was found to occur in the PVC/PUR systems based on brittle core materials. In contrast, buckling failures in the top composite skin were observed in the intermediate modulus systems, whereas initial damage in the higher modulus systems took the form of delamination within the top surface skin. Mines et al. [41] showed that a preferential failure mode of sandwich beams for energy absorption is the top skin compressive failure followed by a stable core crushing and then the back face tensile failure. This kind of failure mode occurs mainly in a sandwich beam with cores whose density is relatively high. Mines and Jones [42] suggested that the back face bending failure can be modelled by an elastic-plastic analysis that employs the 'bending hinge' concept in dynamic plastic response of metallic structures. Based on this concept, Li et al. [43] developed an analytical model to predict the behaviour of a simply supported composite sandwich beam subjected to a mass impact at the mid-span at small deflections. The dynamic response corresponding to different intensities is characterised by three regimes, i.e. elastic response regime, core crushing failure regime and final failure regime.

In recent years, increasing efforts have been made to use novel stretching-dominated cores, which have greater stiffness to weight and strength to weight ratios than those of foams. Deshpande and Fleck [44] measured and modelled the collapse responses of full-metal sandwich beams comprising a truss core and either solid or triangulated face-sheets in 3-point bending. It was found that collapse is by four competing mechanisms: face yield, face wrinkling, indentation and core shear, with the active collapse mode dependent upon the beam geometry and yield strain of the material. Upper bound expressions for the collapse loads were given in terms of the effective properties of the faces and core of the sandwich beam. Rathbun et al. [45] measured the bending response of a tetrahedral truss core, and the results demonstrate robust behaviour beyond the limit load. Wicks and Hutchinson [46] conducted a comprehensive study on the optimal design of sandwich beams with a tetrahedral truss core and either solid or triangulated face-sheets. They found that the weight of the optimised beams for a given bending and shear strength was comparable to that for honeycomb-core sandwich beams and stringer-reinforced plates. Wallach and Gibson [47] used experimental and finite element techniques to investigate the stiffness and strength of a double layer grid comprising triangulated faces and a pyramidal truss core. Wang et al. [48] used 3-point bending to test the performance of sandwich beam with the Kagomé core. The basic finding was that, at the equivalent core density, the Kagomé outperforms tetrahedral and pyramidal cores. The major attributes are its isotropy relative to the competing concepts and the suppression of premature softening caused by plastic buckling. Rathbun et al. [49] studied the structural performance of sandwich beams with hollow truss lattice cores made from a ductile stainless steel. The trusses are arranged in an orthogonal (cross-ply) configuration, in either ±45° (diamond) or 0°/90° (square) orientations with respect to the face sheets. The responses in shear, tension and compression, as well as simply supported and fully clamped bending, are measured for specimens with both core orientations. While the two cores perform equally well in compression, the diamond orientation exhibits higher shear strength but lower stretch resistance. Rubino et al. [50] tested the collapse response of steel sandwich beams with a Y-frame core. They found that the high longitudinal shear strength of the Y-frame increases the indentation strength of the Y-frame beams substantially, and for any given indentation depth, the Y-frame sandwich beams absorb significantly more energy than metal foam core sandwich beams of equal mass. To date, very few studies have reported on the low velocity impact behaviour of the sandwich beams with lattice cores.

2.2. SANDWICH PLATES

In general, the performances of sandwich pates under lateral loadings are assessed using two approaches: (1) indentation by a concentrated force and (2) compression by a uniformly distributed pressure.

2.2.1. Indentation

The indentation tests on sandwich structures can be performed by a servo-hydraulic material testing machine (for quasi-static tests) or a drop hammer (for low velocity impact tests), which can produce impacts with the velocity up to 15 m/s. This type of studies is mainly concerned with the structural response, load carrying capacity, failure pattern and energy absorption of the sandwich panels due to indentation damages. The parameters governing the indentation response of sandwich panels may include: the material properties and geometry of the face-sheet and core, shape of projectile, boundary conditions and impact velocity [51]. Figure 5 illustrates the damage evolution of a typical sandwich plate with composite face-sheets and an aluminium honeycomb core [52]. It has been found that the impact failure modes are similar to static indentation failure modes, but the energy absorption in the impact cases is slightly higher [53].

A large amount of research work has been carried out experimentally [52–60] and numerically [54, 55, 61–64], and it is hard to include all of them in this paper.

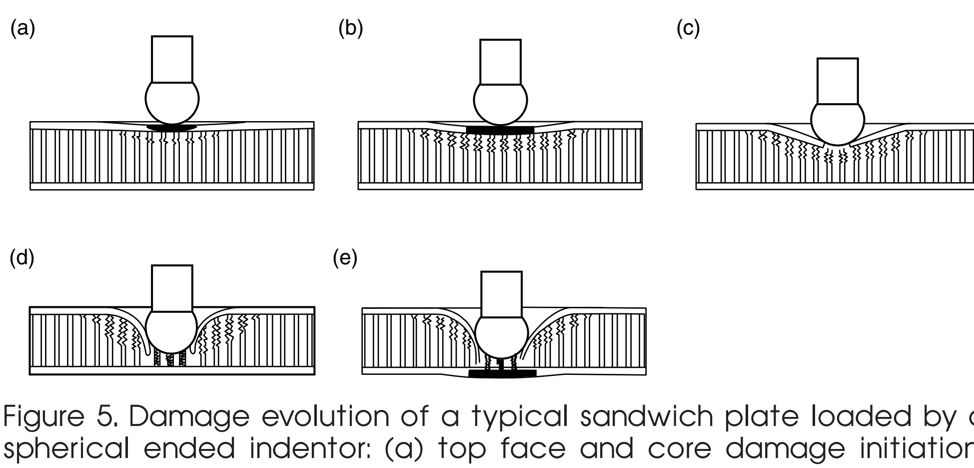

Figure 5. Damage evolution of a typical sandwich plate loaded by a spherical ended indentor: (a) top face and core damage initiation; (b) damage progression; (c) top face fracture; (d) top face penetration and core crushing; (e) Core densification and back face damage initiation (52)

A comprehensive review was given in [65]. As to the analytical solutions for sandwich structures, much fewer investigations have been available, because of the complex interaction between the face sheets and core during deformation and failure. Some recent representative work is briefly summarised here. The mass-spring and energy-balance models are two widely used analytical solutions to study the impact dynamics of foreign objects on composite structures [66]. In the mass-spring model, the sandwich panel were modelled as a discrete dynamic system with equivalent masses and springs/dashpots. There is a combination of bending, shear, membrane and contact springs to calculate the load-deflection response. In the energy-balance model, the kinetic energy of the projectile is equated to the sum of energies due to contact, bending, shear and membrane deformations, and then the maximum deflection and impact force can be estimated. Most of the current analytical models assume elastic behaviour and they are unable to model damage growth. Hoo Fatt and Park [67] used the mass-spring model to predict the low velocity impact response of rigidly supported, two-sided clamped, simply supported and four-sided clamped composite sandwich panels. The composite sandwich panels had orthotropic face-sheets and were symmetric. The analysis was in terms of local indentation and structural global deformations, and the strain rate effect was considered as well. The same authors [68] developed another analytical model to calculate the impact force and velocity for several damage initiation modes: tensile and shear fracture of the top face-sheet, core shear failure and tensile failure of back face. Similar analytical and numerical models for low velocity impact response and damage initiation were proposed by the other group of researchers using the energy-balance model [69, 70]. A more detailed and dedicated review on the analytical modelling can be seen in [69].

It should be emphasized that to date the indentation studies on the sandwich panels have been limited to the conventional structures with composite faces and polymeric/honeycomb cores. No work on the metallic foam and novel lattice structures has been reported.

2.2.2. Uniaxial Compression

The stress-strain response and damage modes of sandwich structures can also be identified by uniaxial compression tests under a uniform loading in the transverse direction. It is a commonly used method to assess the loading carrying capability and energy absorbing performance of sandwich structures with novel cores (shown in Figure 6).

Wadley and co-workers [71–73] conducted transverse compression tests on sandwich plates with either solid or hollow aluminium alloy lattice trusses, as shown in Figure 6(a). A similar lattice structure made of titanium was studied by Moongkhamklang et al. [74]. Figure 7 illustrates the through thickness compressive stress–strain response of a specimen with solid aluminium lattice core. Following an initial linear response, a peak was observed in the compressive stress that coincided with initiation of the buckling of the lattice truss members and the formation of a plastic hinge near the centre of the truss members. Continued loading resulted in core softening up to an engineering strain of 0.25, at which point the load-carrying capacity increased rapidly as the deformed trusses made contact with the face-sheets. During the core-softening phase, small fractures were observed to form on the tensile stressed side of the trusses. These were first seen at strains of between 0.10 and 0.12. No failures at the truss face-sheet nodes were observed during any of the tests. Compared with the solid trusses, hollow truss structures significantly increase the second moment of inertia of the trusses and thus their resistance to elastic or plastic buckling.

Zupan et al. [75] investigated the plastic collapse behaviour of aluminium egg-box panels with two core geometries (Figure 6(b)) for unconstrained, bonded and constrained uniaxial

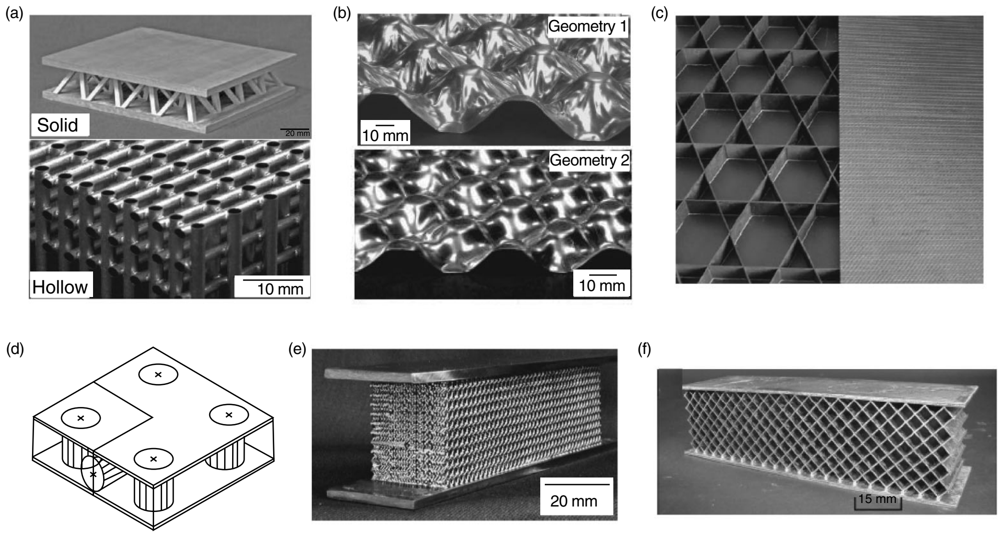

Figure 6. Several sandwich plates with novel cores: (a) solid and hollow lattice truss structures; (b) egg-box structures; (c) Kagomé grid cores reinforced by carbon fibers; (d) FRP tubes reinforced structure; (e) woven core structure; (f) corrugated core structure. Detail references are given in the text

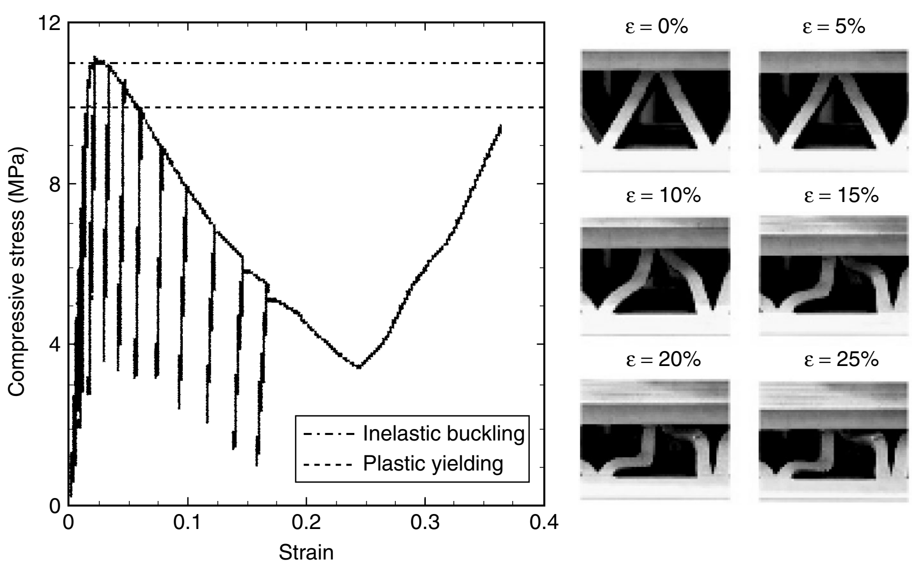

Figure 7. Compressive stress vs. strain response and photographs of the lattice deformation at strain levels of 0%, 5%, 10%, 15%, 20% and 25%. Predictions of the stress for inelastic buckling and plastic yielding of the trusses are also shown (74)

compression. The results showed that collapse strength and energy absorption were sensitive to the level of in-plane constraint, with collapse dictated either by plastic buckling or by a travelling hinge mechanism, and the energy absorption capacity of the egg-box structure was comparable to that of metallic foams. Figure 6(c) shows a structure with carbon fiber reinforced lattice grids tested by Fan et al. [76]. It was found that the grid core was much stiffer and stronger than foams and honeycombs, and buckling and debonding dominated the mechanical behaviour of the sandwich structures. Another type of composite sandwich panels reinforced with internal FRP tubes (Figure 6(d)) was experimentally and numerically studied by Mamalis et al. [77, 78]. The failure of the specimens took place initially by collapse of the reinforcing transverse FRP tubes in axial compression and followed by transverse compression of the longitudinal reinforcing element, which resulted in delamination and fracture of this tube and finally densification of the core. It was concluded that the FRP tubes improved significantly the stiffness and the crash energy absorption features of the tested sandwich panels. A novel stainless steel woven/textile-core sandwich panel, as shown in Figure 6(e), has been studied by several researchers [79–81], and the analytical model to predict the stiffness and peak strength of core structure was developed. The results show that this structure was a good energy absorber, and the damage modes and energy dissipating performance were highly dependent on the boundary conditions. The deformation processes and stress-strain behaviours of the woven cores without and with face-sheets are indicated in Figures 8 (a) and (b), respectively. The initial nonlinear-crushing stress was about 5 MPa for both cases. The sustained crushing stress was about 7 and 10 MPa for the cases without and with face-sheets, respectively. Significant strain hardening occurs for the configuration with face-sheets. The absorbed energy within the core at maximum strain was 9.8 J/cm^2 (7.2 J/g) for the configuration with face sheets and 6.3 J/cm^2 (4.6 J/g) for the configuration without. The crushing response depended on the presence or absence

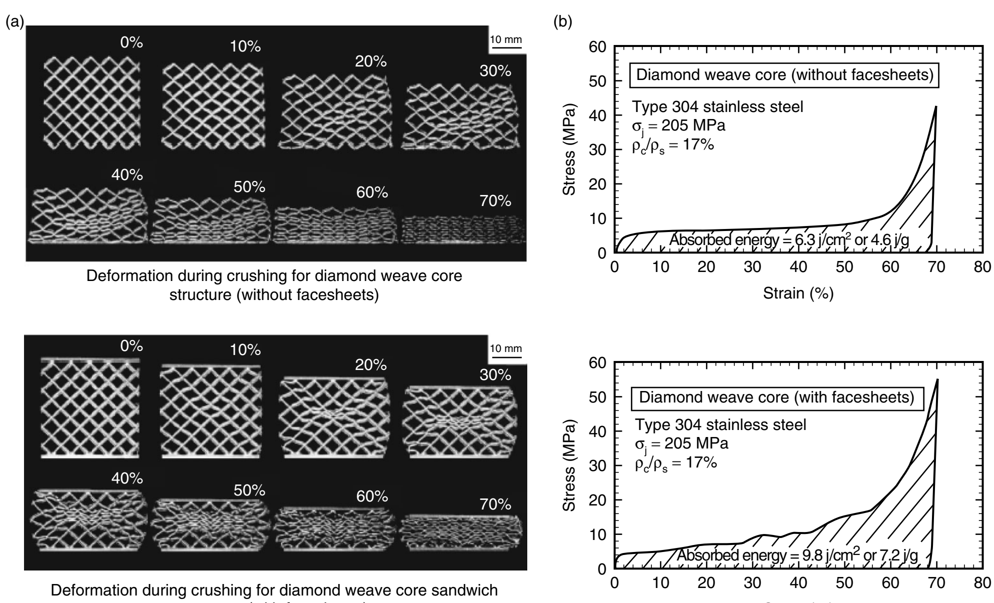

Figure 8. deformation processes and stress-strain behaviour of the woven cores without and with face-sheets (81)

of face-sheet constraint. When face-sheets are present, the crushing is initiated by collapse of the center diamond followed by the development of deformation bands, stretching from the corners to the centre, which is a 'global' failure mode. Absent face-sheets to control the deformation a localised diagonal shear band of deformed trusses was formed, eventually leading to final collapse of the core. Hence one can conclude that perfectly bonded woven structures can absorb more energy than unconstrained structures.

Cote et al. [82] studied the compressive behaviour of a 2D corrugated core structure (Figure 6(f)), which exhibits peak stress followed by a strong softening response. Densification of the core was not investigated because the corrugations on the inner surfaces of the face-sheets permitted nominal compressive strains larger than 1. Based on the concept of corrugated plate core, a hierarchical corrugated structure has been developed [83]. Unlike the common (first order) corrugated core promising solid struts, a hierarchical (second order) core has struts of truss core sandwich columns, as illustrated in Figure 9(a). In second order trusses, elastic buckling and yielding of the larger and smaller struts, shear buckling of the larger struts, and wrinkling of the face sheets of the larger struts have been identified as the six competing modes of failure, as shown in Figure 9(b). The analytical analysis revealed that second order trusses made from structural alloys have significantly higher compressive and shear collapse strengths than their equivalent mass first order counterparts for relative densities less than about 5%.

Apart from physical compressive experiments, computational and analytical models have been proposed for the stiffness, plastic collapse and buckling behaviours of several other core topologies [45, 84–86]. Another purpose of compressive experiments is to test the compression-after-impact (CAI) strength of sandwich structures, as one of the main drawbacks of sandwich structures is the loss of load carrying capacity due to indentation damages [87]. A few studies have been performed on different structures, and the conclusions vary significantly with specific panel configurations, material properties and loading conditions

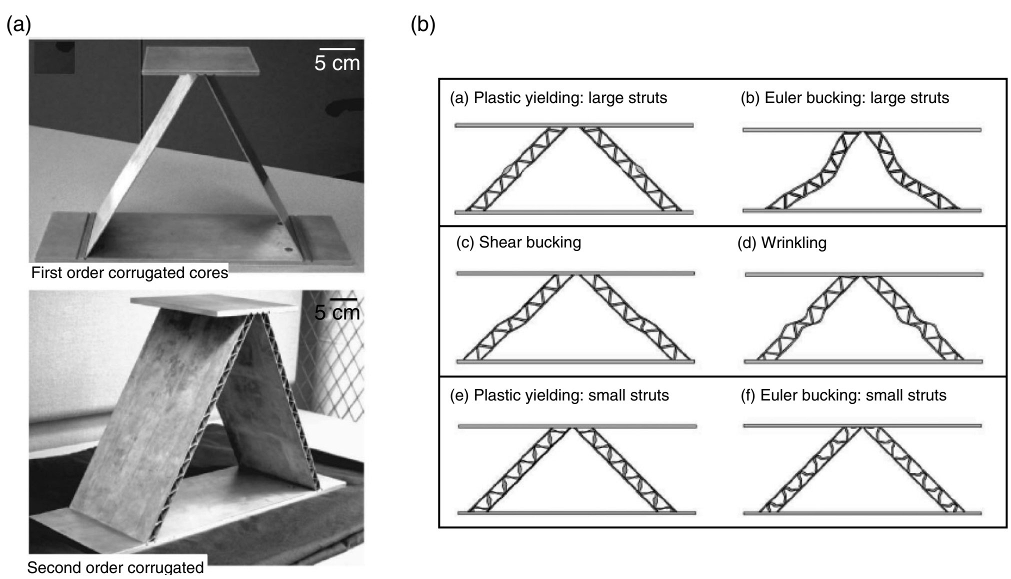

Figure 9. First and second order corrugated cores and schematic drawings of the failure modes in the second order corrugated core (83)

[87–89]. Axial compression tests can also be conducted in the edgewise direction to measure the in-plane strength of sandwich columns/plates/beams, and identify their failure modes [90–92]. Generally, the operative mechanism depends on the properties of the bulk material and geometry of the sandwich structures.

3. BALLISTIC IMPACT PERFORMANCE

The concept of a 'ballistic impact' defined here is an impact resulting in complete penetration of the structure. Based on the scope of impact velocities, the ballistic tests may be implemented by a drop hammer or a gas gun setup with different strikers. A detailed review of equipments is seen in [94]. To quantify the ballistic tests, two critical parameters are usually analysed to evaluate the perforation resistant behaviour and energy dissipating performance of the targets: (1) ballistic limit (V_b), which is defined as the velocity when the projectile is either stuck in the back face or else exits with the negligible velocity; and (2) perforation energy (E_p), which is essentially the energy loss of the projectile during perforation. In this section, the review is presented in terms of damage modes of the structures, impact velocity effect and analytical models.

3.1. DAMAGE MODES

Damage behaviour of sandwich structures in perforation is complex and depends on the material and structural configuration of the specific application, as well as the shape of the indenter noses. Kepler [95, 96] tested the perforation resistance of simply supported square sandwich panels with fiber reinforced polymeric composite faces and a PVC foam core using MTS and drop hammers with conical, round and flat ended impactors. Three visible damages were measured and quantified, which included delaminations between the lamina of the face-sheets, debonding between core and inner face-sheet, and core cross-cracking and punching. It was found that the shape of impactors has significant effects on the penetration resistance and energy absorption. The largest amount of core compression takes place in the cylindrical volume defined by the impactor diameter. The energy required for compression depends on the impactor type. The pointy tips push the material sideways, whereas the blunt tips push the material in the impact direction. Different mechanisms would result in different amount of energy dissipation. More discussions on the effect of impactors can be seen in [97–100, 109].

The high velocity perforation response of novel FML-reinforced skin/aluminium foam core sandwich structures has been studied using a gas gun by Villanueva and Cantwell [101]. The structures exhibited a number of energy absorbing mechanisms such as fibre-matrix delamination, longitudinal splitting and fibre fracture in the composite skins and indentation, progressive collapse and densification in the aluminium foam. Impact testing of such sandwich structures has shown that these hybrid materials offer specific perforation energies approximately 23% higher than their plain composite counterparts having similar composite volume fractions.

Recently, the ballistic performance of the structure with novel stretching-dominated cores under high velocity impact has been studied [102, 103]. In [102], the stainless steel pyramidal lattice core sandwich panels were found to have a much higher ballistic resistance than the aluminum alloy panels on a per volume basis but the ballistic energy absorption of the aluminum structures was slightly higher on a per unit mass basis. The ballistic performances of the monolithic and sandwich panels were almost identical though the failure mechanics of these two types of structures were rather different. At high impact velocities, the monolithic plates failed by ductile hole enlargement. By contrast, only the proximal face sheet of the sandwich plate undergoes this type of failure. The distal face sheet failed by a

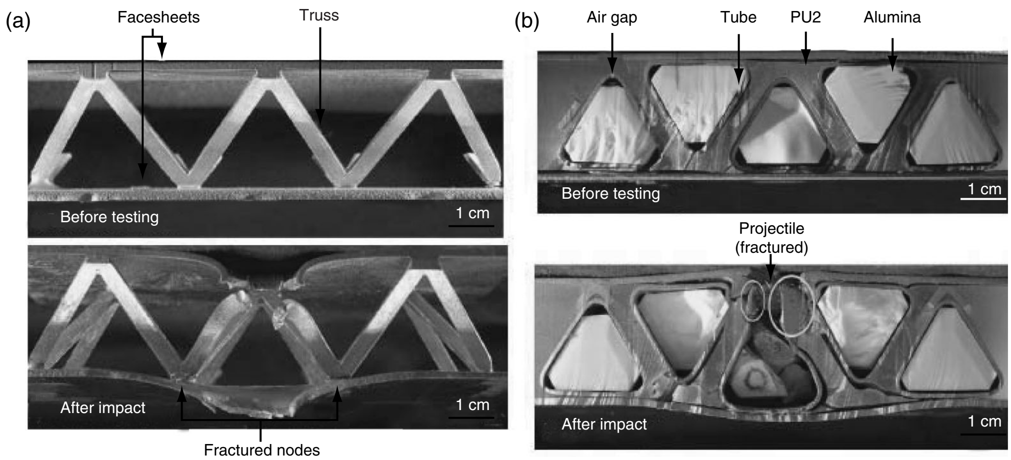

Figure 10. Cross-sections of pyramidal lattice cores before and after ballistic impact: (a) filled with air; (b) filled with PU2 (102, 103)

petalling mode over the entire velocity range investigated here, as shown in Figure 10(a). In [103], an air filled pyramidal lattice was compared with some polymer infiltrated lattices. It has been shown that the air filled pyramidal lattice structure can be relatively easily penetrated by such projectiles when the face sheets are thin and the core relative density is low (<3%). Some polymer infiltrated 'hybrid' lattices have greatly improved ballistic resistance compared to their unfilled counterparts. A system consisting of metal encapsulated ceramics in a polymer infiltrated lattice (PU2) was found to have the much higher ballistic resistance, as illustrated in Figure 10(b).

3.2. VELOCITY EFFECT

In some cases, the energy required for penetration under impact loading is significantly higher than in the static case. The effect of perforation velocity on this energy enhancement phenomenon has been studied extensively.

Goldsmith et al. [104] executed an experimental study of the ballistic limits of aluminium honeycomb sandwich panels with aluminium alloy face-sheets using projectiles in the form of spheres, or 60° cylindro-conical bullets and blunt nosed cylinders. It was found that the ballistic limit for each size and shape of penetrator exhibited a nearly linear relation with the areal density of the target. However, the smaller projectiles evidenced a greater slope than the larger sizes. The variation of terminal velocity as a function of initial velocity beyond the ballistic limit followed the standard pattern of a short, concave-downward curve, where the perforation resistance of the target was dominant, followed by a linear region where the piercing process represented a small fraction of the total initial kinetic energy of the striker. Mines et al. [105] tested the low velocity perforation performance of two sandwich constructions, namely woven glass vinylester skins with Coremat core and woven glass epoxy pre-preg skins with honeycomb core. Results have shown that the density of the core influenced the progression of failure and that higher impact velocity increased the energy absorption capabilities of the panels. The core crush dominated overall energy absorption and that the increase in perforation energy form static to dynamic loading can be due to a change in deformation geometry as well as material strain rate effects. Some suggestions have been made on how to increase panel perforation energy, i.e. the use of high ductility skins, the use of multiple layers and the tailoring of the multi-axial crush behaviour of the core. Roach et al. [106, 107] studied the relation of energy absorption and damage of sandwich panels with GRP laminate skins and laminate skins and a closed cell PVC core perforated by a flat ended solid cylindrical indenter in both quasi-static and impact loading conditions. It has been found that the ratio of dynamic penetration energy to static penetration energy rises rapidly initially with velocity, plateauing at about 100 m/s. More energy is required to penetrate laminates than to penetrate laminate with a core foundation. There exists a linear correlation between the impact energy and the area of damage, at all velocities, and that this correlation is most accurate for the foam-backed laminates.

Zhao et al. [108] used an instrumented Hopkinson pressure bar as a perforator and at the same time a measuring device, as shown in Figure 11(a). The approach aimed at a high quality piercing force record during the whole perforation process, which is a weak point of common freeflying projectile-target testing schemes. This new testing arrangement allows for the measurement of piercing force–displacement curves under quasi-static and impact loadings of sandwich samples, which is made of Cymat foam cores and aluminium alloy sheets as top and bottom skins (Figure 11(b)). Compared with quasi-static top skin peak loads (the maximal load before the perforation of top skins) obtained under same geometric and clamping conditions in Figure 11(c), a significant enhancement under impact loading (25%) of the top skin peak load was found. However, the used foam core and skin sheet were known and have been confirmed to be hardly rate sensitive by separate tests on foam cores as well as on the skin sheets. A possible explanation of these puzzling results is following: the foam core under the perforator was locally more compressed under impact loading because of the inertia effect. As the used foam cores has a quite important strain hardening behaviour, the strength of foam cores before the failure of the top skin is higher than that under quasi-static loading, which leads to an increase of the top skin peak load under impact loading. Tests on a uniformly pre-compressed sandwich sample exhibit indeed higher top skin peak loads, which also supports this aforementioned concept. Such behavior of aluminium foam core sandwich panels has been observed in a similar ballistic test by Hou et al. [109].

3.3. ANALYTICAL MODELS

A few analytical models have been developed to predict the ballistic limit and energy absorption of the sandwich structures during perforation.

Wen et al. [99] and Reid and Wen [100] performed penetration tests on the FRP laminates and two FRP skinned sandwich panels. Simple analyses using spring models have been developed to describe the initial failure of the top skin of sandwich panels loaded quasi-statically by flat ended and hemispherical ended indenters. Formulae for the loads corresponding to the three principal failure modes, that is, indentation, core shear and global bending, and the transition equations between these modes have also been given in the quasi-static case. The experimental data have been used to derive an empirical equation that predicts the ballistic limit and perforation energies of fibre-reinforced plastic laminates and sandwich panels with such laminates as skins and with foam cores subjected to quasi-static and impact loading by a hemispherical ended indenter.

Hoo Fatt and co-workers [111–113] proposed a theoretical model for the perforation of sandwich panels with E-glass/polyester composite skins and an aluminium honeycomb core. The complete process of perforation was split into three stages:

Stage I – Initiation of the top face-sheet failure. Top face-sheet failure occurs due to local indentation. Face-sheet indentation is modelled by considering a rigid indenter pressing into a composite membrane resting on a rigid plastic foundation.

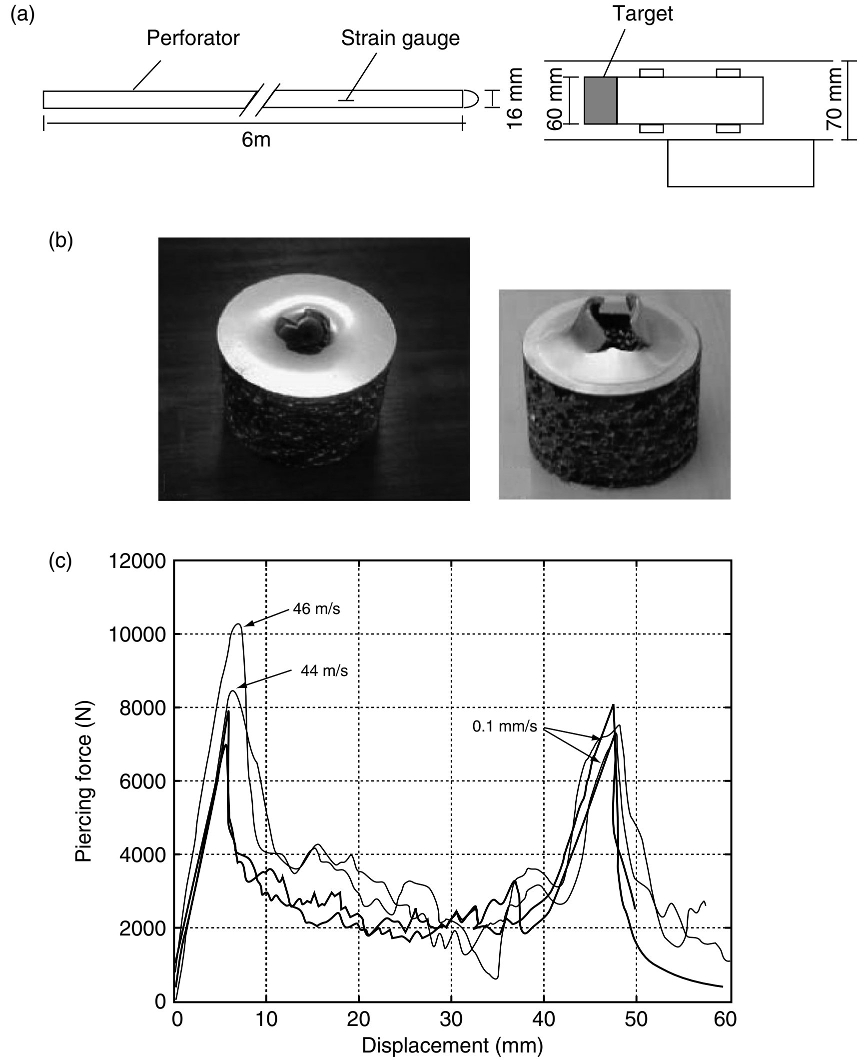

Figure 11. Experimental setup, specimens and result: (a) Hopkinson pressure bar; (b) top and bottom skins and a specimen after quasi-static perforation; (c) quasi-static and impact piecing force vs displacement curves (108)

Stage II – Penetration of the top face-sheet and punch shear failure of the core. This stage begins when the indenter has caused initial tensile failure on the top face-sheet. Damage initiation is in the form of a cross-hair fracture which leads to petaling under the projectile.

Stage III – Bottom face-sheet tensile failure. After core crushing failure, the indentation load will be transferred to the bottom face-sheet. The bottom face-sheet/core debonding occurs instantaneously and extensively. The resistance force comes from the friction between the indenter and the core, and the membrane stretching of the bottom face-sheets. The resistance from the top face-sheet vanishes at the end of stage II.

The three-stage perforation model was considered in the dynamic analysis and conservation of energy was combined with the equations of motion to obtain the ballistic limit.

Skvortsov et al. [114] developed a mathematical model to describe the penetration in sandwich panels for intermediate and high-range incident velocities, where it was assumed that the perforation energy can be divided into two parts:

$$E_{abs} = E_{dam} + E_{pan} \tag{2}$$

where E_{dam} is the energy absorbed due to damage of sandwich composites, i.e. matrix cracking, core crushing, debonding, delamination and fibre failure. E_{pan} is the energy absorption due to panel elastic response (deformation and motion). Based on the similar energy partition, Velmurugan et al. [115] proposed another simple analytical model to predict the impact response of a sandwich structure, including the ballistic limit.

4. DYNAMIC EFFECTS

Crushing at high strain rates may significantly raise the resistance and energy absorption of the cellular cores of sandwich constructions. The dynamic behaviour of these cores at high strain rates is of current interest of academia. In general, a Hopkinson/Kolsky bar apparatus is used to investigate intermediate deformation rates; while high deformation rates are examined using a light gas gun. It has been found [116–120] that besides material strain rate sensitivity, two other dynamic effects can significantly affect the core performance: (1) inertial resistance of the core to the motion of the front face-sheet and the consequent plastic wave propagation in the core; and (2) inertial stabilization of the core ligaments that can delay the onset of buckling, thereby maintaining the effective strength of the core to much larger crushing strains than under quasi-static crushing. Core ligament stabilization is also understood to lead to significant increase in the energy-absorption capacity of the lattice core sandwich plates.

Lee et al. [116] tested the quasi-static, intermediate and high strain rate behaviour of the solid stainless steel pyramidal truss core shown in Figure 6(a), using a miniature loading stage, a Kolsky bar and a gas gun, respectively. Figure 12 is a plot of measured nominal stress–nominal strain signatures. In all cases, after an initial nominal stress increase, the load reaches a peak value and then drops. This load–displacement behaviour is characteristic of structures prone to instability collapse. A close examination of Figure 12 reveals significant rate effects as manifested by differences in peak compressive nominal stress. The peak load in the gas gun loading is the largest, followed by the peak load measured in the Kolsky bar experiments, and as expected, the peak load measured in the quasi-static experiments was the smallest. In terms of nominal stress, the quasi-static peak stress is 4.0–4.2 MPa, about 60% the peak stress recorded in the Kolsky bar experiments (6.4 MPa) and three times smaller than the peak stress measured in the gas gun experiments (9.6–12.0 MPa). In the quasi-static and Kolsky bar experiments, the post-peak load smoothly decreases to what seems to be a steady-state value, which is similar in both loading rates. On the other hand, several instabilities (load drops) at different displacement levels are recorded in the gas gun loading. Comparison of areas under load–deformation responses shows that the energy absorbed up to a strain of 0.4 in the gas gun experiment is more than twice the energy absorbed in the quasi-static and Kolsky bar experiments. The failure patterns in the quasi-static and intermediate strain rate cases were similar, but the

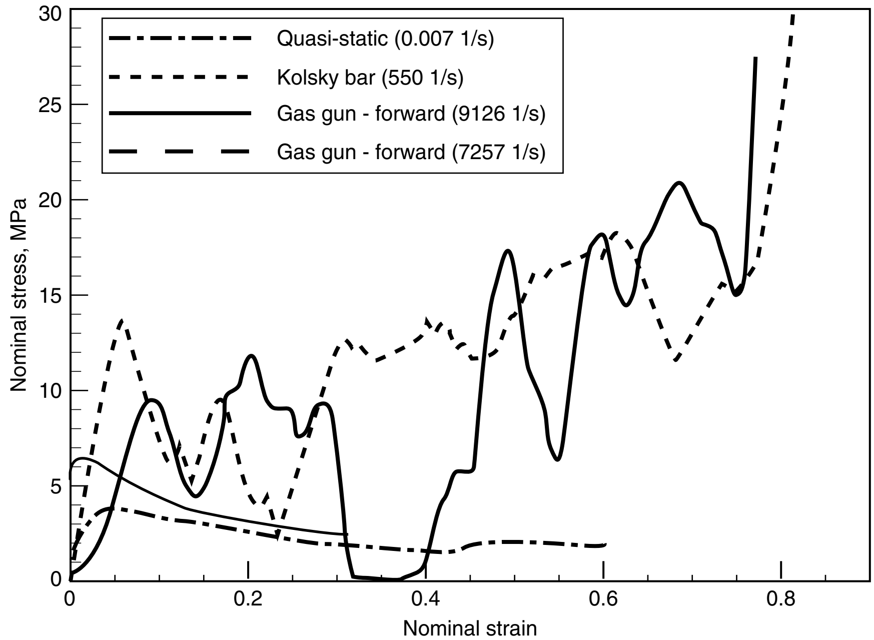

Figure 12. Stress-strain curves of pyramidal truss core being crushed at different strain rates (116)

deformation mode at high strain rate was quite different, with the members deforming plasticity in a more localised fashion. This is the case because propagation of the plastic wave delays overall buckling of the member.

Tang et al. [117] investigated the same pyramidal truss core sandwiches made of aluminium alloys using a SPHB together with a special cooling tank between the incident and transmitter bars, to understand the phenomenon of buckling in truss structures as a function of loading rates and test temperature. Lower test temperatures were found to produce significant effects on the force–displacement curves of the truss structures. Reduced test temperatures increase the crush resistance and mechanical energy absorption capability of the truss structures tested. Tilbrook et al. [118] compared the dynamic out-of-plane compressive responses of stainless steel corrugated (Figure 6(f)) and solid Y-frame (Figure 6(a)) sandwich cores for impact velocities ranging from quasi-static values to 200 m/s. The stresses on both the front and rear faces of the sandwiches were measured in the dynamic tests using a direct impact Kolsky bar. Two distinct mechanisms govern the dynamic response of the cores: (i) inertial stabilization of the webs against buckling and (ii) plastic wave effects. The front and rear face peak stresses remain approximately equal for impact velocities less than 30 and 60 m/s for the Y-frame and corrugated sandwich cores, respectively. Inertial stabilization of the webs against buckling is the dominant dynamic strengthening mechanism at these lower velocities. However, inertial stabilization has a smaller effect on the bending-dominated Y-frame cores compared to the stretching-dominated corrugated cores. At higher impact velocities, plastic wave effects within the core members result in the front face stresses increasing with increasing velocity while the rear face stresses remain approximately constant.

Using the same setups described in [116], Lee et al. [119] studied deformation rate sensitivity of an open cell aluminium foam and the aluminium woven core structure shown in Figure 6(e). Woven textile materials exhibited moderate dependence of strength on the deformation rate in comparison with open cell materials. At low strain rates, the collapse zone was observed in the central region with shear bands at +/–45° in orientation. At high strain rates, collapse occurred adjacent to the impact surface and propagated through the specimen in the direction of impact. McKown et al. [120] employed a drop tower and explosive to produce intermediate and high rates loadings on a similar woven core structures made of stainless steel. At the highest strain rates (10^3/s), the deformation mode remained unchanged from the quasi-static and intermediate rates. They suggested the increase in strength of the lattice is due to the material's own property, rather than the shock wave enhancements.

5. BLAST LOADING RESPONSE

In recent years, sandwich structures have been increasingly used for blast protection, due to enhanced chance of blast threats. Therefore it is essential to have a deeper insight into their shock resistant behaviour, failure mechanism and energy absorbing performance.

When an explosive charge is detonated in air or water, the rapid expansion of the detonation products creates a shock wave with discontinuities in pressure density, temperature and velocity. The free-field pressure pulse approaching the target can be described by

$$p(t) = p_0 e^{-t/t_0} \tag{3a}$$

where t_0 is the characteristic decay time and p_0 is the peak pressure. Then the impulse per unit area on a stationary, rigid target, I_0, transported by the pressure pulse is given by

$$I_0 = 2\int_0^\infty p(t)\,dt = 2p_0 t_0 \tag{3b}$$

The factor of 2 arises in Eq. (3b) due to full reflection of the pressure wave.

A brief overview of blast loading of sandwich structures in terms of experiments, analytical modelling and numerical simulations has been presented by the authors in [121]. In this paper, a more detailed review is given with the supplement of some most recent advances.

5.1. EXPERIMENTAL INVESTIGATIONS

5.1.1. Using an Aluminium Foam Cylinder to Simulate an Impulsive Load

The use of metal foam projectiles to simulate water and air shock loading upon a structure has been developed by Radford et al. [122]. The technique is simple and safe to use in a laboratory setting and produces pressure histories representative of those observed in fluid shock loading. In this approach, metal foam projectiles are fired from a gas gun at high velocities, as illustrated in Figure 13(a). This procedure produces a 'patch' loading over a narrow range relative to the support span. The pressure versus time history exerted depends upon the foam projectile density ρ_p, length l_0, compressive stress versus strain response of the foam, and projectile velocity v_0. The analysis suggested that metal foam projectiles exert a rectangular pressure versus time pulse of magnitude

$$p_0 = \sigma_c + \frac{\rho_p v_0^2}{\varepsilon_D} \tag{4a}$$

and duration

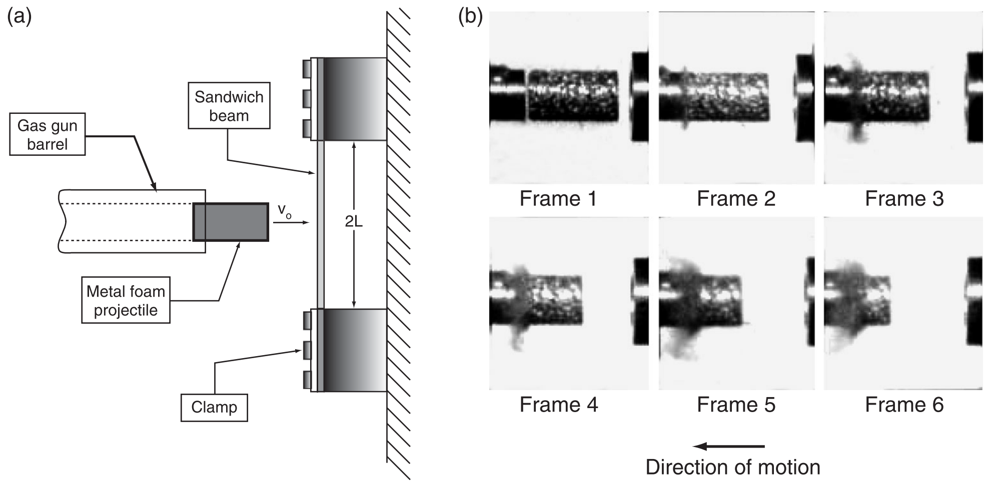

Figure 13. Using an aluminium foam cylinder to simulate an impulsive load: (a) experimental setup; (b) a high-speed photographic sequence of metal foam impacting a Kolsky pressure bar [122]

$$\tau = \frac{l_0 \varepsilon_D}{v_0} \tag{4b}$$

on a rigid stationary target. Here, σ_c and ε_D are the plateau stress and nominal densification strain of the foam, respectively. This pressure versus time history, however, is sensitive to the structural response of the target: a decrease in the mechanical impedance of the target leads to a decrease in the applied pressure and to an increase in the pulse duration. Figure 13(b) shows a high-speed photographic sequence of a direct impact experiment. The foam projectile was of length L = 50 mm; of relative density 11% and was fired at a velocity of 381 m/s. The exposure time of each photograph was 4 ms and the inter-frame times were 20 ms. The sequence of images reveals the propagation of a plastic shock wave from the impact face of the foam projectile. The distal portion of the projectile remains almost undeformed prior to arrival of the compression wave. The shock event occurs as a planar wave and direct observations after the impact event confirmed that the foam deformation occurred with negligible radial expansion. A cloud of dust is evident in the photographs, and was due to the brittle fragmentation of the foam cells at the shock front.

This approach has been applied to test the blast loading performance of a wide range of sandwich structures: sandwich plates with steel faces and aluminium foam core [123]; sandwich plates with steel faces and steel pyramidal and square honeycomb cores [124]; sandwich beams comprising steel faces and steel pyramidal cores, steel corrugated cores and an aluminium alloy metal foam [125]; sandwich beams with steel faces and steel square honeycomb cores [126]; glass fibre-vinylester sandwich beams with PVC foam cores [125]; and steel sandwich beam and rectangular plates with Y-frame and corrugated cores [128, 129].

Deshpande et al. [130] and Mori et al. [131] used shock tube techniques to measure the dynamic structural response under a realistic, although scaled, fluid-structure interaction with a water borne shock. In the setup, a scaled structure is fixed at one end of the steel tube and a water piston seals the other end. A flyer plate impacts the water piston and produces an exponentially-decaying pressure history in lieu of blast loading caused by explosive detonation. The pressure induced by the flyer plate propagates and imposes an impulse to the structure (panel specimen), whose response elicits water cavitation.

5.1.2. Air Explosion Tests

Dharmasena et al. [132] conducted air blast tests at three levels of impulse load on the steel square honeycomb core sandwich panels and solid plates with the same areal density. Impulse was varied by changing the charge weight of the explosive at a constant standoff distance. At the lowest intensity load, significant front face bending and progressive cell wall buckling were observed at the center of the panel closest to the explosion source. Cell wall buckling and core densification increased as the impulse increased. In the tests, only final deflections of the plates were measured. Karagiozova et al. [133] used a ballistic pendulum system to test the response of circular flexible sandwich-type panels subjected to air blast loading. The specimens had steel face-sheets and an aluminium honeycomb core, which were not adhered together. It was found that the velocity was attenuated through the core thickness, which influences the transmitted stress pulse to the back plate, determines the permanent deflections.

Zhu et al. [134] conducted a large number of experiments to test the structural response of blast loaded square sandwich panels comprising aluminium alloy face sheets and a core made of either hexagonal aluminium alloy honeycomb. The test program was divided into four groups, each of which was designed to identify the effect of key parameters, such as cell size and foil thickness of the honeycomb, face-sheet thickness and mass of charge. In the tests, a four-cable ballistic pendulum system (Figure 14) with a laser displacement transducer was used to measure the impulse imparted on the panel, and a PVDF pressure gauge recorded the pressure–time history at the centre point of the specimen's front face.

The experimental results were classified into two categories: (1) quantitative results, which include the impulse on sandwich panel, permanent mid-point deflection of the back face and pressure–time history at the centre point of front face; and (2) deformation/failure modes of specimen observed in the tests. It has been shown that specimens with thicker face sheets, a higher density core and loaded by larger charges tend to have localised deformation

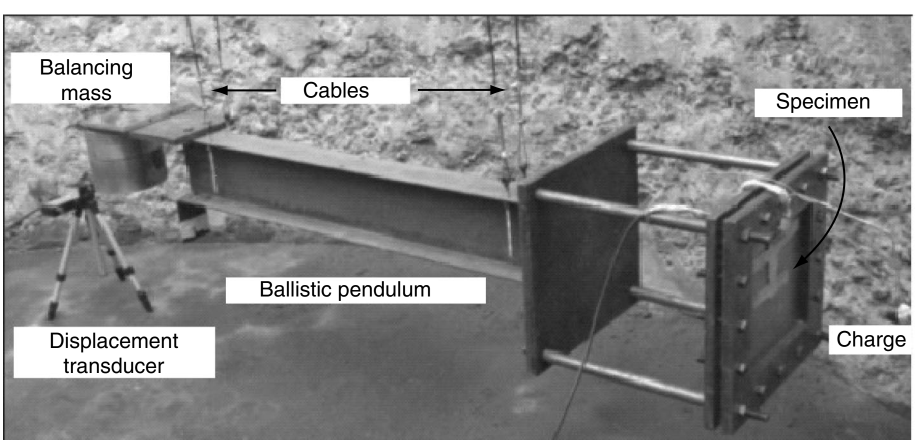

Figure 14. A four-cable ballistic pendulum system for air blast tests (134)

on the front face, and those with thinner skins and a sparse core and subjected to lower level shocks are prone to deform globally. Based on the quantitative analysis, it has also been found that the face-sheet thickness and relative density of core structure can affect the back face deformation greatly. By adopting thicker skins and honeycomb cores with higher relative density, the deflection of back face can be reduced. Also, for a given panel configuration, it is evident that the back face deflection increases with impulse, approximately linearly.

Recently, the same facility was used to test the blast loaded curved sandwich panels with two aluminium face-sheets and an aluminium foam core [135]. Initial radius of curvature was found to have significant influence on the deformation/failure behaviour. Firstly, it changed the reflective angle of the reflected blast wave, and resulted in a reduction of the impulse acting on the front face of sandwich panels. Secondly, it led to a new failure pattern, wrinkling of the back face sheet of the sandwich panels, which was not observed in the flat sandwich panels. Thirdly, it changed the deformation regimes in terms of bending and stretching.

Schenker et al. [136] experimentally studied the effectiveness of aluminum foams as a protection layer for reinforced concrete (RC) plates subjected to blast loading. Fewer cracks were observed in protected RC plates. Structures can be better protected by the scarifying layer of aluminum foams against explosive loadings.

5.1.3. Underwater Explosion Tests

A multilayered pyramidal lattice structure constructed from stainless-steel (Figure 15(a)) subjected to underwater blast was investigated by Wadley et al. [137] using a special setup given in Figure 15(b). The lattice was found to crush in a progressive manner by the sequential (cooperative) buckling of truss layers. During dynamic loading, sequential buckling of the truss layers was manifested as a series of transmitted pressure pulses measured at the back face of the test samples. The sequential buckling extended the duration of the back face pressure–time waveform and significantly reduced the transmitted pressure measured at the back face. The impulse transmitted to the structure was found to be about

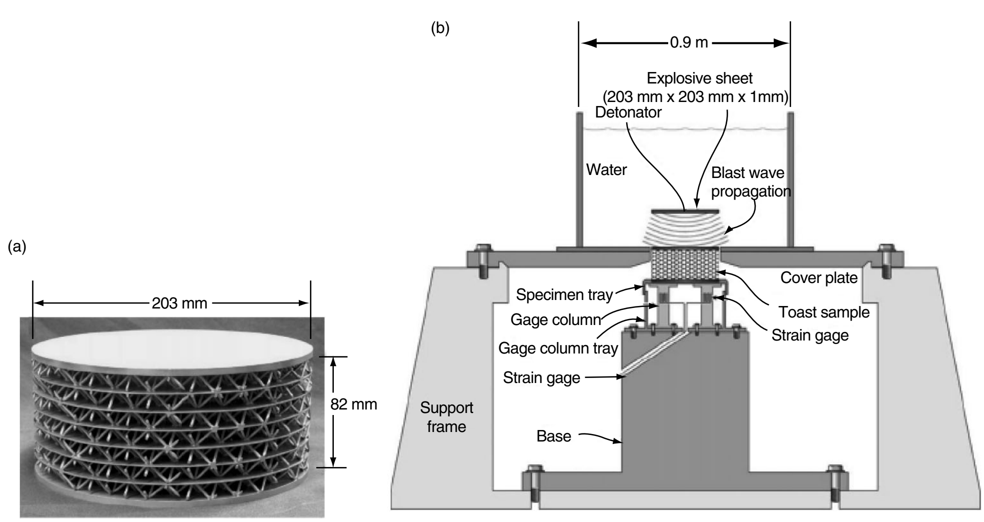

Figure 15. Underwater blast tests of a multilayered pyramidal lattice structure: (a) specimen; (b) setup [137]

28% less than that predicted by analytic treatments of the fluid-structure interaction for fully supported structures. Wei et al. [138] used the same setup to study the resistance of monolithic metallic and sandwich panels to localised spherical and planar impulsive sources. Comparisons based on the central point displacement revealed that the honeycomb panel is superior to a solid plate when subjected to a planar impulse, but inferior when localised. The insights gained from an interpretation of these results were used to demonstrate that a new design with a doubly-corrugated soft core outperforms solid plates both for planar and localized impulses.

5.2. DIMENSIONLESS ANALYSES

Dimensionless analyses were conducted by Xue and Hutchinson [139–141] to investigate the performance of monolithic and sandwich plates subject to air and water impulses. Their analyses were based on some assumptions:

(1) The blast loading in air is idealised into an impulse, i.e. the period of pressure is zero;

(2) In the deformation of a sandwich structure, when its back face deflection is still less than about the sandwich thickness, the response of the sandwich plate is dominated by bending. The top face-sheet experiences in-plane compression while the bottom face undergoes in-plane tension. As even larger deflections develop, stretching takes over and the in-plane stresses become tensile in both faces. The solid plate undergoes a similar transition from bending to stretching but at much smaller deflections that are on the order of its thickness;

(3) The second order effects, such as strain hardening, material strain rate effects, specific fracture modes and dynamic strengthening of the core are disregarded.

A small set of important dimensionless parameters has been identified for monolithic plates and sandwich structures with pyramidal truss, corrugated and square honeycomb cores. Based on the dimensionless parameters identified, a limited study of weight optimization was carried out using FE simulation for each of the core types with respect to the respective geometric parameters, including core and face sheet thickness, core member aspect ratios and relative density. It was concluded that a well-designed sandwich plate can sustain much larger blast impulses than a solid plate of the same weight. If the blast medium is water, fluid–structure interaction can reduce the momentum imparted to a sandwich plate by almost a factor of two relative to that imparted to a solid plate of the same weight, and, consequently, the relative benefit of the sandwich plate is significantly enhanced over its solid counterpart.

5.3. ANALYTICAL SOLUTIONS

5.3.1. Three-Phase Analytical Models

A series of analytical models have been developed by Fleck and co-workers, to predict the dynamic response of sandwich beams and circular sandwich panels under a uniform shock loading [142, 143] or a non-uniform one over a central patch [144]. The sandwich structures comprise steel face-sheets and cellular solid cores, with ends fully clamped. The response to shock loading is measured by the permanent transverse deflection at the centre of the structures. In the models, a number of approximations have been made to make the problem tractable to an analytical solution. Principally, these are

(i) the 1-D approximation of the shock events;

(ii) separation of the phases of the response into three main sequential phases (shown in Figure 16):

Phase I: This is actually a 1-D air-structure interaction process during the blast event, resulting in a uniform velocity of the outer face-sheet.

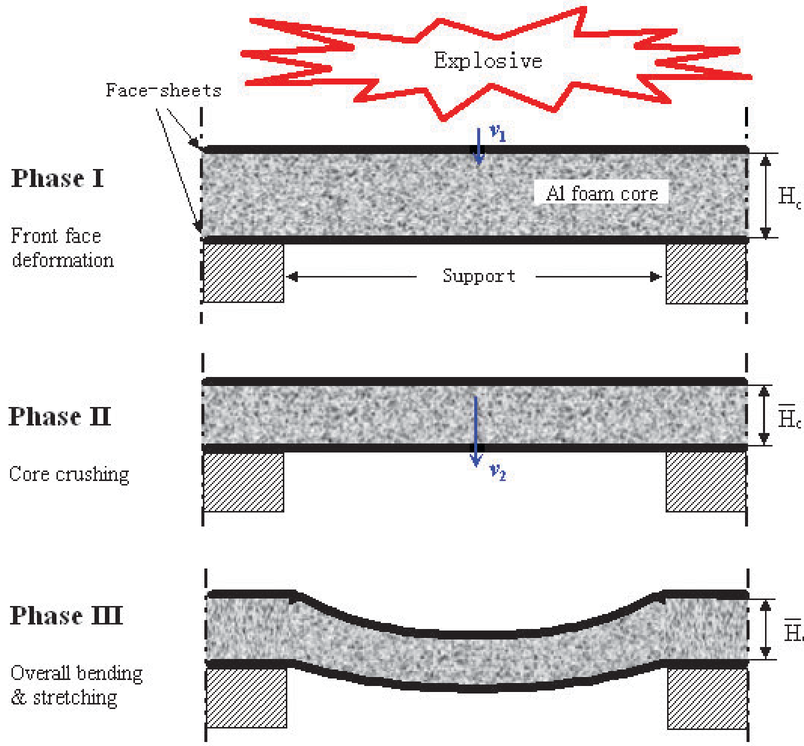

Figure 16. Three phases in the response of a sandwich panel subjected to the blast loads (146)

Phase II: The core crushes and the velocities of the faces and core become equalised by momentum sharing.

Phase III: This is the retardation stage at which the structure is brought to rest by plastic bending and stretching. The problem under consideration here is turned into a classical one for monolithic beams or plates.

(iii) neglect of the support reaction during the shock event and during the core compression phases;

(iv) a highly simplified core constitutive model wherein the core is assumed to behave as an ideally plastic locking solid with a homogeneous deformation pattern; and

(v) neglect of the effects of strain hardening.

Despite these approximations, the analysis has been shown to compare well with corresponding numerical simulations [141–145]. The analytical solution for rectangular sandwich panels under blast loading is much more complex, because of their non-axisymmetric geometry, for which the principal stress directions are unknown in advance, a complete theoretical analysis of the dynamic response is rather complicated, especially when deformation is large.

Based on this three-phase procedure, Zhu et al. [146] developed a design-oriented approximate solution for blast loaded rectangular sandwich panels, which is excellent for predicting maximum permanent deflections, but gives no predictions of displacement-time history. The response in the last phase was considered using either small deflection or large deflection theories, respectively, based on the extent of panel deformation. The analysis was based on an energy balance with assumed displacement fields. In the small deflection analysis, bending is the main energy dissipation mechanism and stretching can be neglected; the kinetic energy is assumed to be dissipated solely at the plastic hinge lines generated. In the large deflection analysis, on the other hand, stretching plays a key role in the deformation mechanism and bending effect can be ignored. The residual kinetic energy is dissipated in the continuous deformation fields. In both cases, the contribution of core in the last phase can be disregarded. By equating the kinetic energy acquired to the plastic strain energy produced in the structure, the permanent maximum deflections of the face-sheets were obtained. The analytical model was validated by comparing the predictions with the experimental data as well as the theoretical calculations based on the analytical model for circular sandwich plates.

More recently, another theoretical model was proposed by authors to predict the dynamic response of square sandwich panels with cellular cores, i.e. not only the final deflection, but also the response time [147]. In the model, the cellular core was assumed to have a progressive deformation mode in crushing with the longitudinal core strength unaffected by compression, and an energy dissipation rate-based approach was proposed to calculate the effective dynamic transverse plateau stress, through the stress-strain curves obtained from the standard uniaxial compression tests with the strain rate effect considered. A newly developed yield surface [148] was used for the sandwich cross-section with different core strengths. By adopting an energy dissipation rate balance approach and the new yield surface, the upper (inscribing yield locus) and lower bounds (circumscribing yield locus) of the maximum permanent deflections and response time corresponding to the inscribing and circumscribing yield loci were obtained. The normalised maximum central deflection of the back face and structural response time according to the circumscribing yield locus are written as

$$\bar{W}_0 = \frac{W_0}{\bar{L}} = \hat{c}\frac{\alpha_1}{\alpha_2}\left[\left(1+\frac{2}{3}\frac{\alpha_2 Z_n}{\alpha_1^2\alpha_3}\right)^{1/2} - 1\right] \tag{5a}$$

$$\bar{T} = \frac{T}{\bar{L}}\sqrt{\sigma_Y^f/\rho_f} = \sqrt{\frac{\alpha_3}{6\alpha_2}}\tan^{-1}\left(\frac{2}{3}\frac{\alpha_2 Z_n}{\alpha_1^2\alpha_3}\right)^{1/2} \tag{5b}$$

where $\hat{c} = \bar{H}_c/\bar{L}$ with $\bar{H}_c$ and $\bar{L}$ being the final thickness of core and half side length of the square plate; $\hat{h} = \bar{h}/(1-\varepsilon_c)$; $\alpha_1 = 4\hat{h}(1+\hat{h})+\bar{\sigma}$; $\alpha_2 = \bar{\sigma}+2\hat{h}$; $\alpha_3 = \left[2\hat{h}+\bar{\rho}/(1-\varepsilon_c)\right]$, with $\bar{h}$, $\bar{\sigma}$ and $\bar{\rho}$ being the face-core thickness ratio, core-face longitudinal tensile strength ratio and core-face density ratio, respectively. ε_c is the compressive strain of core in the transverse direction. It can be found that α_1, α_2 and α_3 actually reflect the effect of plastic bending, stretching and dimensionless mass, respectively. Z_n is herein defined as 'sandwich damage number', which can be used to assess the dynamic plastic response of sandwich structures, and $Z_n = \dfrac{\bar{I}^2}{\sigma_Y^f\rho_f\bar{H}_c^2}\dfrac{1}{\hat{c}^2}$, where σ_Y^f and ρ_f are yield strength and density of face-sheet material. $\bar{I}$ is normalised impulse per unit area. It should be noted that in this model, the longitudinal strength of core was assumed not affected by compression (termed as Assumption 1); while in the model by Qiu et al. for circular plates [143], the plastic membrane force was assumed unchanged and thus the longitudinal strength would increase (termed as Assumption 2). If Assumption 1 is adopted for the model of circular plates, it is interesting to find that it has completely the same expression with the formulae of square panels, i.e. Eq. (5). When $\varepsilon_c = 0$ and $\bar{\rho} = 1$, Eq. (5) reduces to the analytical model for monolithic square plates developed by Jones [149].

5.3.2. Coupling Effects Between the Phases

The analytical models described above all assumed that the three phases are decoupled each other. However, due to different ratios of core-face strength and fluid-solid interaction in the water explosion, coupling effects may take place between Phases I and II or II and III.

Deshpande and Fleck [150] examined the significance of coupling between the fluid–structure interaction phase I and the core compression phase II. They demonstrated that the traditional analysis based upon a free-standing front face-sheet underestimates by 20–40% the transmitted momentum for sandwich beams comprising high strength cores. McShane et al. [151] performed FE simulations with the couplings between the three stages of response switched on and off and demonstrated that the enhanced performance for sandwich beams observed in their study is primarily a result of coupling between core compression in phase II and combined beam bending and stretching in phase III of the sandwich beam response. This coupling is most significant in beams with a core of low transverse strength. Liang et al. [152] have elucidated two types of sandwich response and labelled them as (1) strong core and (2) soft core type responses (Figure 17). The mid-span velocity versus time histories of the front and back faces of the strong core response is sketched in Figure 17(a): the front and back face velocities equalise early in the deformation history. Subsequently, the faces share a common velocity–time response and both the face-sheets are brought to rest during the subsequent sandwich mode of bending/stretching. In contrast, in the soft core type behaviour (Figure 17(c)), the back face begins to decelerate while the core is still compressing. They suggested that the optimal performance of sandwich beams is attained for soft core designs. They showed that a core with a low transverse strength reduces the transmitted impulse during the initial fluid–structure interaction stage. Tilbrook et al. [153] conducted a similar study, demonstrating that the value of the transverse core strength that minimises the back face deflection also minimises the support reactions. However, the optimal core strength depends on the level of blast impulse, with higher strength cores required for greater blasts.

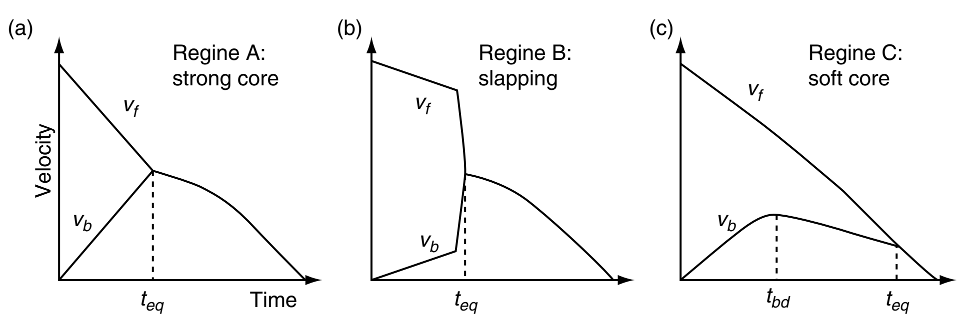

Figure 17. Velocity versus time histories of the mid-span of the front and back faces for three types of sandwich response: (a) 'strong core', (b) 'slapping' occurs for full core densification at supports before velocity equalisation and (c) "soft core" type sandwich response (152)

5.4. FE SIMULATIONS

Blast testing is extremely expensive and time consuming, while FE simulations, if adequately formulated and accurately realised, help to greatly reduce the volume of laboratory and field blast tests. FEA offers the possibility to predict distribution of stress/strain and wave propagation that are difficult to be measured experimentally, and give the detailed process of internal structural deformation and failure which can be hardly observed. Besides, FEA can be used to identify the influence of critical parameters on the structural behaviour under certain conditions. Due to the highly transient and nonlinear nature of Explosion Mechanics, the corresponding FEA often involves the dynamic problems associated with large deformation, high pressure/temperature/strain rate, failure of material, solid-fluid interaction etc. Finite element models solve the problems by discretising the related equations which govern the process of explosion and consequent structural response, and setting some initial conditions.

5.4.1. Basic Formulations

Generally, most of the Explosion Mechanics problems involving large deformations and solid/liquid interactions are described by three basic formulations, i.e. (1) Lagrangian methods; (2) Eulerian methods; and (3) hybrid methods.

- Lagrangian methods

  In these methods, the mesh is attached with the mass particles and moves and deforms with the material. They can handle moving boundaries or multiple materials very naturally, but perform poorly or even fail when large deformations take place, due to the distortion of the elements.
- Eulerian methods

  These methods, on the contrary, use a fixed mesh, which does not move with materials. They are suitable to solve the problems with large deformations, but have difficulties when the computing domain includes multiple materials or free surfaces.
- Hybrid methods

  The hybrid methods seek a compromise between the Lagrangian methods and Eulerian methods. A typical hybrid method is ALE (Arbitary-Lagrangian-Eulerian) method, which allows the mesh within any material region to be continuously adjusted in predefined ways as a calculation proceeds, thus providing a continuous and automatic rezoning capability. Therefore, it is suitable to use an ALE approach to analyse solid and fluid motions when material strain rate is large and significant (for example, the detonation of explosive and volume expansion of explosion products).

5.4.2. Modelling Blast Loads

- Defining the pulse-time curve or velocity field directly

  The idea of directly defining the pulse-time curve or velocity field on the structure is quite straightforward and may be the easiest way to model blast loads. However, the coupling effects of the loads and structures, such as the change of structural curvature and shock wave reflections, are not considered. Therefore, sometimes the simulation performance of this method is not satisfactory. Vaziri and Hutchinson [154] compared the effects of the approaches of applied pressure and prescribed velocity in the intense air shock simulations. They suggested that there is little difference between the overall deflection of the bottom face of the sandwich plates from the two approaches. The greatest difference arises in the core crushing. The initial velocity approach can significantly over-estimate core crushing and energy dissipation.

- Defining blast loads using blast pressure functions
  The blast loads can be conveniently calculated using blast pressure functions such as ConWep [155], which was developed by the US Army. The ConWep function can produce non-uniform loads exerted on the top surface of the plates. This blast function can be used in two cases: free air detonation of a spherical charge, and the ground surface detonation of a hemispherical charge. The input parameters include equivalent TNT mass, type of blast (surface or air), detonation location, and surface identification for which the pressure is applied. ConWep calculates the reflected pressure values and applies them to the designated surfaces by taking into account the angle of incidence of the blast wave. It updates the angle of incidence incrementally and thus account for the effect of surface rotation on the pressure load during a blast event. The drawback of ConWep is that it cannot be used to simulate the purely localised impulsive loads produced by explosive flakes or prisms. Some simulation work using ConWep can be found in the literature [132, 156].
- Modelling the explosive as a material
  In this method, the explosive is modelled as a material. When the explosive is detonated, its volume expands significantly and interacts with the structure. The contact force between the expanded explosive product and structure is then calculated [157, 158]. The expansion of the explosive is defined by three parameters: position of the detonation point, burn speed of the explosive and the geometry of the explosive. The explosive materials are usually simulated by the use of the equation of state, which describes the pressure of the detonation.

5.4.3. Modelling the Materials of Targets

- Modelling monolithic metals
  The Johnson-Cook material model is a widely used constitutive relation, which describes plasticity in metals under strain, strain rate, and temperature conditions. If only the strain rate effect is considered, this model can be reduced to another well known material model, namely the Cowper-Symonds relationship, in which the strain rate is calculated for time duration from the start to the point, where the strain is nearly constant from the equivalent plastic strain time history.
- Modelling composite materials
  A large number of computational models have been well established for composite laminates [66], where strain rate effect and failure criteria were defined. Examples of modelling composite face sandwich structures under blast loading can be seen in [159–162].
- Modelling cellular solids
  Periodic cellular materials such as honeycombs and trusses can be either modelled as individual cells or an equivalent solid; while stochastic foams can only be modelled as a solid block. The first approach is generally used to examine the detailed deformation mode of the microstructures, but would be very time-consuming and would not permit an exploration of trends. On the other hand, modelling the core as a solid is more practical where the effective properties of the solid mimic those of the cellular core. A detailed review of constitutive models for cellular materials applicable to structural

impact and shock analyses has been presented by Hanssen et al. [163]. The models have different formulations for the yield surface, hardening rule and plastic flow rule, while fracture is not accounted for in any of them.

5.4.4. Modelling Damage

Damage of material such as ductile tearing or fracture is neglected in most of the simulations. Recently, Vaziri et al. [164] assessed the failure behaviours of steel sandwich beams with either square honeycomb core or folded plate core via numerical simulations. Effect of material properties such as strength, strain hardening and ductility on the necking and subsequent tearing was studied. Zhu et al. [165] performed a similar numerical study on the tearing behaviour of square aluminium sandwich plates with a hexagonal honeycomb core. The emphasis was placed on the effect of structure configuration on the failure response. A pressure-impulse (P-I) diagram was established to describe the dependence of failure modes on the loading conditions.

6. SUMMARY

This paper presents a review on the behaviour of sandwich structures with the core of cellular materials under various loading conditions. Based on the type of microstructures, the cellular materials considered here include metal foams, honeycomb and prismatic materials, as well as truss and textile materials. The loads could be quasi-static compression or indentation, low velocity impact, or highly intense, i.e. ballistic perforation, high speed compression and blast impact. In each type of loading condition, the response of sandwich structures is reviewed, with the focus on their plastic deformation modes and mechanisms, failure evolution and energy absorption capability. The main methodologies applied in this subject, i.e. experimental investigations, analytical modelling and numerical simulations, are also summarised.

ACKNOWLEDGEMENT

The authors wish to acknowledge, with thanks, the financial support from the Australian Research Council through a Discovery Grant. The work was largely conducted when the first author was a post-doctoral fellow at SUT.

REFERENCES

1. Lu G and Yu TX. Energy absorption of structures and materials. Cambridge: Woodhead Publishing Ltd., 2003.
2. Gibson LJ and Ashby MF. Cellular solids: structure and properties, 2nd edition. Cambridge: Cambridge University Press, 1997.
3. Ashby MF, Evans AG, Fleck NA, Gibson LJ, Hutchinson JW and Wadley HNG. Metal foams: a design guide. Oxford: Butterworth-Heinemann, 2000.
4. Degischer H-P, Kriszt B. Handbook of cellular metals: production, processing, applications. Weinheim: Wiley-VCH, 2002.
5. Hexcel Co.. HexWeb® Honeycomb energy absorption system design data, 2005.
6. Wadley HNG. Multifunctional periodic cellular metals. Philosophical Transactions of the Royal Society A, 2006; 364: 31-68.
7. Evans AG, Hutchinson JW, Fleck NA, Ashby MF and Wadley HNG. The topological design of multifunctional cellular metals. Progress in Materials Science, 2001; 46: 309–327.
8. Wadley HNG, Fleck NA and Evans AG. Fabrication and structural performance of periodic cellular metal sandwich structures. Composites Science and Technology, 2003; 63: 2331–2343.

9. Kooistra GW and Wadley HNG. Lattice truss structures from expanded metal sheet. Materials & Design, 2007; 28: 507–514.
10. Deshpande VS, Ashby MF and Fleck NA. Foam topology bending versus stretching dominated architectures. Acta Materialia, 2001; 49: 1035–1040.
11. Wang JG, Sun W and Anand S. A microstructural analysis for crushable deformation of foam materials. Computational Materials Science, 2008; 44: 195–200.
12. Nammi SK, Myler P and Edwards G. Finite element analysis of closed-cell aluminium foam under quasi-static loading. Materials & Design, 2010; 31(2): 712–722.
13. Allen HG. Analysis and design of structural sandwich panels. Oxford: Pergamon Press, 1969.
14. Plantema FJ. Sandwich construction. New York: Wiley Ltd., 1966.
15. Vinson JR. The behavior of sandwich structures of isotropic and composite materials. Lancaster: Technomic Publishing Co., 1999.
16. Zenkert D. An introduction to sandwich construction. Warley: Emas Press, 1995.
17. Daniel IM, Gdoutos EE, Wang KA and Abot JL. Failure modes of composite sandwich beams. International Journal of Damage Mechanics, 2002; 11: 309–334.
18. Daniel IM, Gdoutos EE, Abot JL and Wang KA. Deformation and failure of composite sandwich structures. Journal of Thermoplastic Composite Materials, 2003; 16: 3345–3364.
19. Shipsha A, Hallstrom S and Zenkert D. Failure mechanics and modelling of impact damage in sandwich beams – a 2D approach: Part I – experimental investigation. Journal of Sandwich Structures and Materials, 2003; 5: 7–31.
20. Shipsha A, Hallstrom S and Zenkert D. Failure mechanics and modelling of impact damage in sandwich beams – a 2D approach: Part II – analysis and modelling, Journal of Sandwich Structures and Materials, 2003; 5: 33–51.
21. Lim TS, Lee CS and Lee DG. Failure modes of foam core sandwich beams under static and impact loads. Journal of Composite Materials, 2004; 38(18): 1639–1661.
22. Kiratisaevee H and Cantwell WJ. The failure behavior of aluminium foam sandwich structures based on fiber reinforced thermoplastics. Journal of Sandwich Structures and Materials, 2003; 5: 53–75.
23. Steeves CA and Fleck NA. Collapse mechanisms of sandwich beams with composite faces and a foam core, loaded in three-point bending. Part I: analytical models and minimum weight design. International Journal of Mechanical Sciences, 2004; 46: 561–583.
24. Steeves CA and Fleck NA. Collapse mechanisms of sandwich beams with composite faces and a foam core, loaded in three-point bending. Part II: experimental investigation and numerical modelling. International Journal of Mechanical Sciences, 2004; 46: 585–608.
25. Tagarielli VL, Fleck NA and Deshpande VS. Collapse of clamped and simply supported composite sandwich beams in three-point bending. Composites Part B: engineering, 2004; 523–534.
26. Zhou G, Hill M and Loughlan J. Damage characteristics of composite honeycomb sandwich panels in bending under quasi-static loading. Journal of Sandwich Structures and Materials, 2006; 8: 55–90.
27. McCormack TM, Miller R, Kesler O and Gibson LJ. Failure of sandwich beams with metallic foam cores. International Journal of Solids and Structures, 2001; 38: 4901–4920.
28. Bart-Smith H, Hutchinson JW and Evans AG. Measurement and analysis of the structural performance of cellular metal sandwich construction. International Journal of Mechanical Sciences, 2001; 43: 1945–1963.
29. Chen C, Harte AM and Fleck NA. The plastic collapse of sandwich beams with a metallic foam core. International Journal of Mechanical Sciences, 2001; 43: 1483–1506.
30. Crupi V and Montanini R. Aluminium foam sandwiches collapse modes under static and dynamic three-point bending. International Journal of Impact Engineering, 2007; 34: 509–521.
31. Yu JL, Wang E, Li J and Zheng Z. Static and low-velocity impact bvehavior of sandwich beams with closed-cell aluminium-foam core in three-point bending. International Journal of Impact Engineering, 2008; 35: 885–894.

32. Tagarielli VL, Fleck NA and Deshpande VS. A comparison of the structural response of clamped and simply supported sandwich beams with aluminium faces and a metal foam core. Journal of Applied Mechanics, ASME, 2005; 72: 408–417.

33. Mohan K, Hon YT, Idapalapati S and Seow HP. Failure of sandwich beams consisting of alumina face sheet and aluminum foam core in bending. Materials Science & Engineering A, 2005; 292–301.

34. Qin QH and Wang TJ. An analytical solution for the large deflections of a slender sandwich beam with a metallic foam core under transverse loading by a flat punch. Composite Structures, 2009; 88: 509–518.

35. Yu JL, Wang X, Wei ZG and Wang EH. Deformation and failure mechanism of dynamically loaded sandwich beams with aluminium-foam core. International Journal of Impact Engineering, 2003; 28: 331–347.

36. Hazizan AM and Cantwell WJ. The low velocity impact response of foam-based sandwich structures. Composites Part B: engineering, 2002; 33: 193–204.

37. Hazizan AM and Cantwell WJ. The low velocity impact response of an aluminium honeycomb sandwich structure. Composites Part B: engineering, 2003; 34: 679–687.

38. Villanueva GR and Cantwell WJ. Low velocity impact response of novel fiber-reinforced aluminium foam sandwich structures, Journal of Materials Science Letters, 2003; 22: 417–422.

39. Kiratisaevee H and Cantwell WJ. The impact response of aluminium foam sandwich structures based on a glass fiber-reinforced polypropylene fiber-metal laminate. Polymer Composite, 2004; 25(5): 499–509.

40. Kiratisaevee H and Cantwell WJ. Low-velocity impact response of high-performance aluminium foam sandwich structures. Journal of Reinforced Plastics and Composites, 2005; 24(10): 1057–1072.

41. Mines RAW, Worrall CM and Gibson AG. The static and impact behavior of polymer composite sandwich beams. Composites Part B: engineering, 1994; 25(2): 95–110.

42. Mines RAW and Jones N. Approximate elastic-plastic analysis of the static and impact behavior of polymer composite sandwich beams. Composites Part B: engineering, 1995; 26(12): 803–814.

43. Li QM, Ma GW and Ye ZQ. An elastic-plastic model on the dynamic response of composite sandwich beams subjected to mass impact. Composite Structures, 2006; 72: 1–9.

44. Deshpande VS and Fleck NA. Collapse of truss core sandwich beams in 3-point bending. International Journal of Solid Structures, 2001; 38: 6275–6305.

45. Rathbun HJ. Wei Z, He MY, Zok FW, Evans AG, Sypeck DJ and Wadley HNG. Measurement and simulation of the performance and a lightweight metallic sandwich structure with a tetrahedral truss core. Journal of Applied Mechanics, ASME, 2004; 71: 368–374.

46. Wicks N and Hutchinson JW. Optimal truss plates. International Journal of Solid Structures, 2001; 38: 5165–5183.

47. Wallach JC and Gibson LJ. Mechanical behavior of a three-dimensional truss material. International Journal of Solid Structures, 2001; 38: 7187–7196.

48. Wang J, Evans AG, Dharmasena K and Wadley HNG. On the performance of truss panels with Kagomé cores. International Journal of Solid Structures, 2003; 40: 6981–6988.

49. Rathbun HJ, Zok FW, Waltner SA, Mercer C, Evans AG, Queheillalt DT and Wadley HNG. Structural performance of metallic sandwich beams with hollow truss core. Acta Materilia, 2006; 54: 5509–5518.

50. Rubino V, Deshpande VS and Fleck NA. The collapse response of sandwich beams with a Y-frame core subjected to distributed and local loading. International Journal of Mechanical Sciences, 2008; 50: 233–246.

51. Abrate S. Impact on composite structures. Cambridge: Cambridge University Press; 1989.

52. Raju KS, Smith BL, Tomblin JS, Liew KH and Guarddon JC. Impact Damage Resistance and Tolerance of Honeycomb Core Sandwich Panels. Journal of Composite Materials, 2008; 42(4): 385–412.

53. Goldsmith W and Sackman JL. An experimental study of energy absorption in impact on sandwich plates. International Journal of Impact Engineering, 1992; 12(2): 241–262.

54. Rizov V, Shipsha A and Zenkert D. Indentation study of foam core sandwich composite panels. Composite Structures, 2005; 69: 95–102.

55. Meo M, Vignjevic R and Marengo G. The response of honeycomb sandwich panels under low-velocity impact loading. International Journal of Mechanical Sciences, 2003; 47: 1301–1325.

56. Dear JP, Lee H and Brown SA. Impact damage processes in composite sheet and sandwich honeycomb materials. International Journal of Impact Engineering, 2005; 32; 130–154.

57. Schubel PM, Luo JJ and Daniel IM. Low velocity impact behavior of composite sandwich panels. Composites Part A: applied science and manufacturing, 2005; 36: 1389–1396.

58. Schubel PM, Luo JJ and Daniel IM. Impact and post impact behavior of composite sandwich panels. Composites Part A: applied science and manufacturing, 2007; 38: 1051–1057.

59. Zhou G, Hill M and Hookham N. Investigation of parameters governing the damage and energy absorption characteristics of honeycomb sandwich panels. Journal of Sandwich Structures and Materials, 2007; 9: 309–342.

60. Park JH, Ha SK, Kang KW, Kim CW and Kim HS. Impact damage resistance of sandwich structure subjected to low velocity impact. Journal of Materials Processing Technology, 2008; 201: 425–430.

61. Kärger L, Baaran J and Te·mer J. Efficient simulation of low-velocity impacts on composite sandwich panels. Computers & Structures, 2008; 86: 988–996.

62. Nguyen MQ, Jacobs SS, Thomson RS, Hachenberg D and Scott ML. Simulation of impact on sandwich structures. Composite Structures, 2005; 47: 217–227.

63. Palazotto AN, Herup EJ, Gummadi LNB. Finite element analysis of low-velocity impact on composite sandwich plates. Composite Structures 2000; 49: 209–227.

64. Besant T, Davies GAO, Hitchings D. Finite element modelling of low velocity impact of composite sandwich panels. Composites Part A: applied science and manufacturing, 2001; 32: 1189–1196.

65. Tomblin J, Lacy T, Smith B, Hooper S, Vizzini A and Lee S. Review of damage tolerance for composite sandwich airframe structures. Federal aviation administration report No. DOT/FAA/AR-99/49, 1999.

66. Abrate S. Localized impact on sandwich structures with laminated facings. Applied Mechanics Review, 1997; 50(2): 69–82.

67. Hoo Fatt MS and Park KS. Dynamic models for low-velocity impact damage of composite sandwich panels – Part A: Deformation. Composite Structures, 2001; 52: 335–351.

68. Hoo Fatt MS and Park KS. Dynamic models for low-velocity impact damage of composite sandwich panels – Part B: Damage initiation. Composite Structures, 2001; 52: 353–364.

69. Foo CC, Seah LK and Chai GB. Low-velocity impact failure of aluminium honeycomb sandwich panels. Composite Structures, 2008; 85: 20–28.

70. Foo CC, Chai GB and Seah LK. A model to predict low-velocity impact response and damage in sandwich composites. Composites Science and Technology, 2008; 68: 1348–1356.

71. Kooistra GW, Deshpande VS and Wadley HNG. Compressive behavior of age hardenable tetrahedral lattice truss structures made from aluminium. Acta Materialia, 2004; 52: 4229–4237.

72. Queheillalt DT, Murty Y and Wadley HNG. Mechanical properties of an extruded pyramidal lattice truss sandwich structure. Scripta Materialia, 2008; 58: 76–79.

73. Queheillalt DT and Wadley HNG. Cellular metal lattices with hollow trusses. Acta Materialia, 2005; 53: 303–313.

74. Moongkhamklang P, Elzey DM, and Wadley HNG. Titanium matrix composite lattice structures. Composites Part A: applied science and manufacturing, 2008; 39: 176–187.

75. Zupan M, Chen C and Fleck NA. The plastic collapse and energy absorption capacity of egg-box panels. International Journal of Mechanical Sciences, 2003; 45: 851–871.

76. Fan HL, Meng FH and Yang W. Sandwich panels with Kagome lattice cores reinforced by carbon fibers. Composite Structures, 2007; 81: 533–539.

77. Mamalis AG, Manolakos DE, Ioannidis MB, Papapostolou DP, Kostazos PK and Konstantinidis DG. On the compression of hybrid sandwich composite panels reinforced with internal tube inserts: experimental. Composite Structures, 2002; 191–199.

78. Mamalis AG, Manolakos DE, Ioannidis MB and Papapostolou DP. Finite element modeling of the crushing response of composite sandwich panels with FRP tubular reinforcements. International Journal of Crashworthiness, 2006; 11(2): 177–188.

79. Zupan M, Deshpande VS and Fleck NA. The out-of-plane compressive behaviour of woven-core sandwich plates. European Journal of Mechanics A/Solids, 2004; 23: 411–421.

80. Sypeck DJ. Cellular truss core sandwich structures. Applied Composite Materials, 2005; 12: 229–246.

81. Caulfield J, Karlsson AM and Sypeck DJ. Crushing of a textile core sandwich panel. AIAA Journal, 2006; 44(6): 1339–1344.

82. Cote F, Deshpande VS, Fleck NA and Evans AG. The compressive and shear responses of corrugated and diamond lattice materials. International Journal of Solids and Structures, 2006; 43: 6220–6242.

83. Kooistra GW, Deshpande VS and Wadley HNG. Hierarchical corrugated core sandwich panel concepts. Journal of Applied Mechanics, ASME, 2007; 74: 259–268.

84. Pedersen CBW, Deshpande VS and Fleck NA. Compressive response of the Y-shaped sandwich core. European Journal of Mechanics A/Solids, 2006; 25: 125–141.

85. Hyun S, Karlsson AM, Torquato S and Evans AG.. Simulated properties of Kagomé and tetragonal truss core panels. International Journal of Solids and Structures, 2003; 40: 6989–6998.

86. Wicks N and Hutchinson JW. Performance of sandwich plates with truss cores. Mechanics of Materials, 2004; 36: 739–751.

87. Shipsha A and Zenkert D. Compression-after-impact strength of sandwich panels with core crushing damage. Applied Composite Materials, 2005; 12: 149–164.

88. Davies GAO, Hitchings D, Besant T, Clarke A, Morgan C. Compression after impact strength of composite sandwich panels. Composite Structures, 2004; 63: 1–9.

89. Lacy TE and Hwang Y. Numerical modeling of impact-damaged sandwich composites subjected to compression-after-impact loading. Composite Structures, 2003; 61: 115–128.

90. Cote F, Biagi R, Bart-Smith H and Deshpande VS. Structural response of pyramidal core sandwich columns. International Journal of Solids and Structures, 2007; 44: 3533–3556.

91. Fleck NA and Sridhar I. End compression of sandwich columns. Composites Part A: applied science and manufacturing, 2002; 33: 353–359.

92. Velecela O, Found MS and Soutis C. Crushing energy absorption of GFRP sandwich panels and corresponding monolithic laminates. Composites Part A: applied science and manufacturing, 2007; 38: 1149–1158.

93. Vadakke V and Carlsson LA. Experimental investigation of compression failure mechanisms of composite faced foam core sandwich specimens. Journal of Sandwich Structures and Materials, 2004; 6: 327–342.

94. Kepler J. Equipment for impact testing of sandwich panels. Journal of Sandwich Structures and Materials, 2003; 5: 161–177.

95. Kepler J. Impact penetration of sandwich panels at different velocities – an experimental parameter study: Part I – parameters and results. Journal of Sandwich Structures and Materials, 2004; 6: 357–374.

96. Kepler J. Impact penetration of sandwich panels at different velocities – an experimental parameter study: Part II – interpretation of results and modeling. Journal of Sandwich Structures and Materials, 2004; 6: 379–397.

97. Goldsmith W, Wang GT, Li K and Crane D. Perforation of cellular sandwich plates. International Journal of Impact Engineering, 1997; 19(5-6): 361–379.

98. Roach AM, Evans KE and Jones N. The penetration energy of sandwich panel elements under static and dynamic loading. Part II. Composite Structures, 1998; 42: 135–152.

99. Wen HM, Reddy TY, Reid SR and Soden PD. Indentation, penetration and perforation of composite laminates and sandwich panels under quasi-static and projectile loading. Key Engineering Materials, 1998; 141-143: 501–552.

100. Reid SR and Wen HM. Perforation of FRP laminates and sandwich panels subjected to missile impact. In: Reid SR, Zhou G, editors. Impact behaviour of fibre-reinforced composite materials and structures. Cambridge: Woodhead Publisher Ltd., 2000.

101. Villanueva GR and Cantwell WJ. The high velocity impact response of composite and FML-reinforced sandwich structures. Composites Science and Technology, 2004; 64: 35–54.

102. Yungwirth CJ, Wadley HNG, O'Connor JH, Zakraysek AJ and Deshpande VS. Impact response of sandwich plates with a pyramidal lattice core. International Journal of Impact Engineering, 2008; 35(8): 920–936.

103. Yungwirth CJ, Radford DD, Aronson M and Wadley HNG. Experimental assessment of the ballistic response of composite pyramidal lattice truss structures. Composites Part B: engineering, 2007; 39(3): 556–569.

104. Goldsmith W, Wang GT, Li K and Crane D. Perforation of cellular sandwich plates. International Journal of Impact Engineering, 1997; 19(5-6): 361–379.

105. Mines RAW, Worrall CM and Gibson AG. Low velocity perforation behaviour of polymer composite sandwich panels. International Journal of Impact Engineering, 1997; 21(10); 855–879.

106. Roach AM, Evans KE and Jones N. The penetration energy of sandwich panel elements under static and dynamic loading. Part I. Composite Structures, 1998; 42: 119–134.

107. Roach AM, Evans KE and Jones N. The penetration energy of sandwich panel elements under static and dynamic loading. Part II. Composite Structures, 1998; 42: 135–152.

108. Zhao H., Elnasri I. and Girard Y. Perforation of aluminium foam core sandwich panels under impact loading-An experimental study. International Journal of Impact Engineering, 2007; 34 (7):1246–1257.

109. Hou W, Zhu F, Lu G and Fang DN. Ballistic impact experiments of metallic sandwich panels with aluminium foam core. International Journal of Impact Engineering, 2010; 37: 1045–1055.

110. Wen HM, Reddy TY, Reid SR and Soden PD. Indentation, penetration and perforation of composite laminates and sandwich panels under quasi-static and projectile loading. Key Engineering Materials, 1998; 141-143: 501–552.

111. Hoo Fatt MS and Park KS. Perforation of honeycomb sandwich plates by projectiles. Composites Part A: applied science and manufacturing, 2003; 31: 889–899.

112. Lin C and Hoo Fatt MS. Perforation of sandwich panels with honeycomb cores by hemispherical nose projectiles. Journal of Sandwich Structures and Materials, 2005; 7: 133–172.

113. Lin C and Hoo Fatt MS. Perforation of composite plates and sandwich panels under quasi-static and projectile loading. Journal of Composite Materials, 2006; 40(20): 1801–1940.

114. Skvortsov V, Kepler J and Bozhevolnaya E. Energy partition for ballistic penetration of sandwich panels. International Journal of Impact Engineering, 2003; 28: 697–716.

115. Velmurugan R, Ganesh Babu M and Gupta NK. Projectile impact on sandwich panels. International Journal of Crashworthiness, 2006; 11(2): 153–164.

116. Lee S, Barthelat F, Hutchinson JW and Espinosa HD. Dynamic failure of metallic pyramidal truss core materials – experimental and modeling. International Journal of Plasticity, 2006; 22: 2118–2145.

117. Tang X, Prakash V, Lewandowski JJ, Kooistra GW, Wadley HNG. Inertial stabilization of buckling at high rates of loading and low test temperatures: Implications for dynamic crush resistance of aluminium-alloy-based sandwich plates with lattice core. Acta Materialia, 2007; 2829–2840.

118. Tilbrook MT, Radford DD, Deshpande VS and Fleck NA. Dynamic crushing of sandwich panels with prismatic lattice cores. International Journal of Solids and Structures, 2007; 44: 6101–6123.

119. Lee S, Barthelat F, Moldovan N, Espinosa HD and Wadley HNG. Deformation rate effects on failure modes of open-cell Al foams and textile cellular materials. International Journal of Solids and Structures, 2006; 43: 53–73.

120. McKown S, Shen Y., Brookes WK, Sutcliffe CJ, Cantwell WJ, Langdo GS, Nurick GN and Theobald MD. The quasi-static and blast loading response of lattice structures. International Journal of Impact Engineering, 2008; 35: 795–810.

121. Zhu F and Lu G. A review of blast and impact of metallic and sandwich structures. Electronic Journal of Structural Engineering, 2007; Special Issue: 92–101.

122. Radford DD, Deshpande VS and Fleck NA. The use of metal foam projectile to simulate shock loading on a structure. International Journal of Impact Engineering, 2005; 31: 1152–1171.

123. Radford DD, McShane GJ, Deshpande VS and Fleck NA. The response of clamped sandwich plates with metallic foam cores to simulated blast loading. International Journal of Solids and Structures, 2006; 43: 2243–2259.

124. McShane GJ, Radford DD, Deshpande VS and Fleck NA. The response of clamped sandwich plates with lattice cores to subjected to shock loading. European Journal of Mechanics A/Solids, 2006; 25: 215–229.

125. Radford DD, Fleck NA and Deshpande VS. The response of clamped sandwich beams subjected to shock loading. International Journal of Impact Engineering, 2006; 32: 968–987.

126. Rathbun HJ, Radford DD, Xue Z, He MY, Yang J, Deshpande VS, Fleck NA, Hutchinson JW, Zok FW and Evans AG. Performance of metallic honeycomb-core sandwich beams under shock loading. International Journal of Solids and Structures, 2006; 43: 1766–1763.

127. Tagarielli VL, Deshpande VS and Fleck NA. The dynamic response of composite sandwich beams to transverse impact. International Journal of Solids and Structures, 2007; 44: 2442–2457.

128. Rubino V, Deshpande VS and Fleck NA. The dynamic response of end-clamped sandwich beams with a Y-frame or corrugated core. International Journal of Impact Engineering, 2008; 35(8): 829–844.

129. Rubino V, Deshpande VS and Fleck NA. The dynamic response of clamped rectangular Y-frame and corrugated core sandwich plates. European Journal of Mechanics A/Solids, 2009; 28: 14–24.

130. Deshpande VS, Heaver A and Fleck NA. An underwater shock simulator. Proceedings of the Royal Society A: Mathematical. Physical and Engineering Sciences, 2006; 462: 1021–1041.

131. Mori LF, Lee S, Xue ZY, Vaziri A, Queheillalt DT, Dharmasena KP, Wadley HNG, Hutchinson JW and Espinosa HD. Deformation and facture modes of sandwich structures subjected to under water impulsive loads. Journal of Mechanics and Structures, 2007; 2(10): 1981–2005.

132. Dharmasena KP, Wadley HNG, Xue Z and Hutchinson JW. Mechanical response of metallic honeycomb sandwich panel structures to high-intensity dynamic loading. International Journal of Impact Engineering, 2008; 35(9): 1063–1074.

133. Karagiozova D, Nurick GN, Langdon GS, Chung Kim Yuen S, Chi Y and Bartle S. Response of flexible sandwich-type panels to blast loading. Composites Science and Technology, 2009: 69: 754–763.

134. Zhu F, Zhao LM, Lu G and Wang Z. Deformation and failure of blast-loaded metallic sandwich panels — Experimental investigations. International Journal of Impact Engineering, 2008; 35: 937–951.

135. Shen J, Lu G, Wang Z and Zhao LM. Experiments on curved sandwich panels under blast loading. International Journal of Impact Engineering, 2010; 37: 960–970.

136. Schenker A, Anteby I, Nizri E, Ostraich B, Kivity Y, Sadot O, Haham O, Michaelis R, Gal E and Ben-Dor G. Foam-protected reinforced concrete structures under impact: experimental and numerical studies. Journal of Structural Engineering (ASCE), 2005; 131(8): 1233–1242.

137. Wadley HNG, Dharmasena K, Chen Y, Dudt P, Knight D, Charette R and Kiddy K. Compressive response of multilayered pyramidal lattices during underwater shock loading. International Journal of Impact Engineering, 2008; 35(9): 1102–1114.

138. Wei Z, Deshpande, VS, Evans AG, Dharmasena KP, Queheillalt DT, Wadley HNG, Murty YV, Elzey PK, Dudt P, Chen Y, Knight D and Kiddy K. The resistance of metallic plates to localized impulse. Journal of the Mechanics and Physics of Solids, 2008; 56(5): 2074–2091.

139. Xue Z and Hutchinson JW. Preliminary assessment of sandwich plates subject to blast loads. International Journal of Mechanical Sciences, 2003; 45: 687–705.

140. Xue Z and Hutchinson JW. A comparative study of impulse-resistant metal sandwich plates. International Journal of Impact Engineering, 2004; 30: 1283–1305.

141. Hutchinson JW and Xue Z. Metal sandwich plates optimized for pressure impulses. International Journal of Mechanical Sciences, 2005; 47: 345–569.

142. Fleck NA and Deshpande VS. The resistance of clamped sandwich beams to shock loading. Journal of Applied Mechanics, ASME, 2004; 71: 386–401.

143. Qiu X, Deshpande VS and Fleck NA. Dynamic response of a clamped circular sandwich plate subject to shock loading. Journal of Applied Mechanics, ASME, 2004; 71: 637–645.

144. Qiu X, Deshpande VS and Fleck NA. Impulsive loading of clamped monolithic and sandwich beams over a central patch. Journal of the Mechanics and Physics of Solids, 2005; 53: 1015–1046.

145. Qiu X, Deshpande VS and Fleck NA. Finite element analysis of the dynamic response of clamped sandwich beams subject to shock loading. European Journal of Mechanics A/Solids, 2003; 32: 801–814.

146. Zhu F, Wang Z, Lu G and Zhao LM. Analytical investigation and optimal design of sandwich panels subjected to shock loading. Materials & Design, 2009; 30: 91–100.

147. Zhu F, Wang Z, Lu G and Nurick G. Some theoretical considerations on the dynamic response of sandwich structures under impulsive loading. International Journal of Impact Engineering, 2010; 37: 625–637.

148. Qin QH and Wang TJ. Analytical solution for the large deflection of fully clamped metallic foam sandwich beam. Advanced Material Research, 2008; 33-37: 559–566.

149. Jones N. A theoretical study of the dynamic plastic behaviour of beams and plates with finite-deflections. International Journal of Solids and Structures, 1971; 7: 1007–1029.

150. Deshpande VS and Fleck NA. One-dimensional response of sandwich plates to under water shock loading. Journal of the Mechanics and Physics of Solids, 2005; 53: 2347–2383.

151. McShane GJ, Deshpande VS and Fleck NA. The underwater blast resistance of metallic sandwich beams with prismatic lattice cores. Journal of Applied Mechanics, ASME, 2007; 74: 352–364.

152. Liang Y, Spuskanyuk AV, Flores SE, Hayhurst DR, Hutchinson JW, MeMeeking RM and Evans AG. The response of metallic sandwich panels to water blast. Journal of Applied Mechanics, ASME, 2007; 74: 81–89.

153. Tilbrook MT, Deshpande VS and Fleck NA. The impulsive response of sandwich beams: Analytical and numerical investigation of regimes of behaviour. Journal of the Mechanics and Physics of Solids, 2006; 54: 2242–2280.

154. Vaziri A and Hutchinson JW. Metal sandwich plates subject to intense air shocks. International Journal of Solids and Structures, 2007; 2021–2035.

155. ConWep – Conventional Weapons Effects Program, V 2.0, US Army Engineering Waterways Experimental Station, Vicksburg, MS, USA, 1991.

156. Nemat-Nasser S, Kang WJ, McGee JD, Guo WG and Isaacs JB. Experimental investigation of energy-absorption characteristics of components of sandwich structures. International Journal of Impact Engineering, 2007; 34: 1119–1146.

157. Zhu F, Zhao LM, Lu G and Gad E. A numerical simulation on the blast impact of square metallic sandwich panels. International Journal of Impact Engineering, 2009; 36: 687–699.

158. Zhu F, Zhao LM, Lu G and Wang Z. Structural response and energy absorption of sandwich panels with an aluminium foam core under blast loading. Advances in Structural Engineering, 2008; 11(5): 525–536.

159. Sriram R, Vaidya UK and Kim JE. Blast impact response of aluminum foam sandwich composites. Journal of Materials Science, 2006; 41: 4023–4039.

160. Bahei-El-Din YA and Dvorak GJ. Enhancement of blast resistance of sandwich plates. Composites Part B: engineering, 2008; 39(1): 120–127.

161. Bahei-El-Din YA and Dvorak GJ. A blast-tolerant sandwich plate design with a polyurea interlayer. International Journal of Solids and Structures, 2006; 43: 7644–7658.

162. Bahei-El-Din YA and Dvorak GJ. Behavior of sandwich plates reinforced with polyurethane/polyurea interlayers under blast loads. Journal of Sandwich Structures and Materials, 2007; 9: 261–281.

163. Hanssen AG, Hopperstad OS, Langseth M and Ilstad H. Validation of constitutive models applicable to aluminium foams. International Journal of Mechanical Sciences, 2002; 44: 359–406.

164. Vaziri A, Xue ZY and Hutchinson JW. Performance and failure of metal sandwich plates subjected to shock loading. Journal of Mechanics of Materials and Structures, 2007; 2(10): 1947–1963.

165. Zhu F, Lu G, Ruan D and Shu D. Tearing of metallic sandwich panels subjected to air shock loading. Structural Engineering and Mechanics, 2009; 32(2): 351–370.